Library Copy
RA-A73L87 R.o.d.

CLASSIFIED

CONFIDENTIAL

C2

Copy 45
RM SL54C23

3 1176 00085 7301

NACA

RESEARCH MEMORANDUM

for the

U. S. Air Force

AERODYNAMIC CHARACTERISTICS INCLUDING EFFECTS OF WING FIXES OF A 1/20-SCALE MODEL OF THE CONVAIR F-102 AIRPLANE AT TRANSONIC SPEEDS

By Robert S. Osborne and Dewey E. Wornom

Langley Aeronautical Laboratory
Langley Field, Va.

CLASSIFICATION CHANGED

C-STAR
V. 8, No. 22

11/30/70
B.m.
12/22/70

CLASSIFIED DOCUMENT

This material contains information affecting the National Defense of the United States within the meaning of the espionage laws, Title 18, U.S.C., Secs. 793 and 794, the transmission or revelation of which in any manner to an unauthorized person is prohibited by law.

NATIONAL ADVISORY COMMITTEE FOR AERONAUTICS

WASHINGTON

CONFIDENTIAL

UNCLASSIFIED

~~CONFIDENTIAL~~

CLASSIFICATION CHANGED

NATIONAL ADVISORY COMMITTEE FOR AERONAUTICS

RESEARCH MEMORANDUM

for the

U. S. Air Force

To

authority of C.STAR V.8, No. 22 Date 11/30/70 12/22/70

AERODYNAMIC CHARACTERISTICS INCLUDING EFFECTS OF WING FIXES OF A 1/20-SCALE MODEL OF THE CONVAIR F-102 AIRPLANE AT TRANSONIC SPEEDS

By Robert S. Osborne and Dewey E. Wornom

SUMMARY

Force tests of a 1/20-scale model of the Convair F-102 airplane have been conducted with and without several wing fixes to high angles of attack at Mach numbers from 0.60 to 1.12 in the Langley 8-foot transonic tunnel.

The basic configuration was subject to severe pitch-up at a lift coefficient of approximately 0.6 at high subsonic Mach numbers. The pitch-up was alleviated by 0.25 chord-extensions extending from the 60- or 70-percent-wing-semispan stations to the tips and by leading-edge or chordwise fences located at the 65-percent-semispan stations. Chord-extensions beginning outboard of the 70-percent-wing-semispan station and vortex generators were ineffective. The chordwise fences were also effective in reducing the drag due to lift of the basic configuration.

INTRODUCTION

At the request of the U. S. Air Force, an investigation of the stability, control, and performance characteristics of a 1/20-scale model of the Convair F-102 airplane has been conducted at transonic and supersonic speeds in the Langley 8-foot transonic and 4-foot supersonic tunnels.

The Convair F-102 is an interceptor airplane with a 60° delta wing and no horizontal tail. It was designed for high-altitude flight at supersonic Mach numbers.

~~CONFIDENTIAL~~

UNCLASSIFIED

Results from the tests in the Langley 4- by 4-foot supersonic pressure tunnel at Mach numbers of 1.61 and 2.01 are presented in reference 1. Reported herein are results obtained from the tests in the Langley 8-foot transonic tunnel of the model with no control deflections at Mach numbers from 0.6 to 1.12 for angles of attack up to 34°. Force and moment characteristics are presented for the basic configuration with the ducts open and closed, and, since severe local longitudinal instability or pitch-up indicated the need for a fix, the aerodynamic effects of wing fixes including chordwise extensions, chordwise and leading-edge fences, and vortex generators are shown. Some external flow characteristics are indicated by tuft and schlieren photographs.

SYMBOLS

A_E	duct exit area, sq ft
b	wing span, in.
C_D	external drag coefficient: C_{D_m} with ducts closed and $C_{D_m} - C_{D_I}$ with ducts open
C_{D_I}	internal drag coefficient, D_I/qS
C_{D_m}	measured drag coefficient, D_m/qS
C_{D_o}	drag coefficient at zero lift
$\frac{dC_D}{dC_L^2}$	drag-due-to-lift factor, averaged from $C_L = 0$ to $C_L = 0.3$
C_L	lift coefficient, L/qS
$C_{L_{(L/D)_{max}}}$	lift coefficient for maximum lift-drag ratio
$\frac{\partial C_L}{\partial \alpha}$	lift-curve slope per degree, averaged from $\alpha = 0^{\circ}$ over linear portion of curve

C_m	pitching-moment coefficient, $\frac{M_{cg}}{qS\bar{c}}$
$\frac{\partial C_m}{\partial C_L}$	static-longitudinal-stability parameter, averaged from $C_L = 0$ over linear portion of curve
$\bar{c}$	wing mean aerodynamic chord, in.
c	local chord, in.
D_m	measured drag, lb
D_I	internal drag, $m\left(V_o - V_E\right) - A_E\left(p_E - p_o\right)$, lb
L	lift, lb
$(L/D)_{max}$	maximum lift-drag ratio
M	free-stream Mach number
M_{cg}	pitching moment about center-of-gravity location at $0.275\bar{c}$ and $0.036\bar{c}$ above wing chord plane, in-lb
m	mass flow through inlets, slugs/sec
m_o	mass flow in free-stream tube of area equal to projected inlet area at $\alpha = 0^o$, slugs/sec
m/m_o	inlet mass-flow ratio
P_b	base pressure coefficient, $\frac{p_b - p_o}{q}$
p_b	static pressure at model base, lb/sq ft
p_E	static pressure at duct exit, lb/sq ft
p_o	free-stream static pressure, lb/sq ft
q	free-stream dynamic pressure, lb/sq ft
S	basic wing area including fuselage, sq ft

V_E velocity at duct exit, ft/sec

V_o free-stream velocity, ft/sec

α angle of attack of wing chord line

APPARATUS AND METHODS

Tunnel

The tests were conducted in the Langley 8-foot transonic tunnel which is a dodecagonal slotted-throat, single-return wind tunnel designed to obtain aerodynamic data through the speed of sound while minimizing the usual effects of choking and blockage. The tunnel operates at approximately atmospheric stagnation pressures. Details of test-section design and flow uniformity are available in reference 2.

Model

The 1/20-scale model of the Convair F-102 used in this investigation was supplied by the contractor and is shown in figure 1. Dimensional details of the basic configuration are presented in figure 2 and table I. The axial distribution of cross-sectional area of the model with the ducts open and closed is shown in figure 3.

The delta wing had 60° sweptback leading edges, 5° sweptforward trailing edges, and used NACA 0004-65 (mod.) streamwise airfoil sections with leading-edge radii of 0.18 percent chord (table II). It was constructed with a steel leading edge and a tin bismuth surface formed over a steel core. The fuselage incorporated a 5° drooped nose with probe and a transition ring designed to delay separation behind the nose, a canopy with an optical flat on a 30° leading-edge slope, and twin ram inlets (designed for the J-67 engine) with internal ducting to the model base. The base diameter was enlarged 0.3 inch over that for a true 1/20-scale model in order to insure that the minimum area of the duct system would be at the inlet with the sting in place. For the ducts-closed condition, faired plugs were installed in the inlets. The vertical tail had the same plan form and airfoil sections as the wing semispan and included a flat-plate antenna located just above the rudder.

The wing fixes tested included chordwise extensions, vortex generators, leading-edge fences, and chordwise fences. Dimensional details and location of the fixes on the wings are shown in figure 4 and table I. The chordwise extensions were formed by sliding the portion of the airfoil section ahead of the maximum thickness forward a distance of

25 percent of the local chord and connecting it to the rearward portion with straight-line elements. These fixes extended, respectively, from the 60-, 70-, 75-, and 80-percent-wing-semispan stations to the tips. The vortex generators were attached to the wings at four semispan stations with their chord lines slanted in turn 10° inboard and 15° outboard with respect to the free stream. The leading-edge fences were located at the 65-percent-semispan station and extended around the leading edge from the upper to the lower wing surfaces. The chordwise fences were located at the 65-percent-semispan station and extended from the leading edge to the elevons (79 percent local chord). The fence height from the 10- to 50-percent-chord stations was equal to the maximum local airfoil section thickness.

Model Support System

The model was attached to a strain-gage balance located inside the fuselage. At its downstream end, the balance was attached to a support tube through couplings which were varied to keep the model near the center of the tunnel at all angles of attack. The support tube was fixed axially in the center of the tunnel by two sets of support struts projecting from the tunnel walls. The support system is shown in figure 1.

Measurements and Accuracy

The test Mach number was determined to within ±0.003 from a calibration with respect to the pressure in the chamber surrounding the slotted test section.

Lift, drag, and pitching moment were determined from an internal strain-gage balance. The pitching moment was measured about a center-of-gravity location at 27.5 percent of the mean aerodynamic chord and 3.6 percent of the mean aerodynamic chord above the chord plane. The coefficients for all configurations were based on the wing area and mean aerodynamic chord of the basic configuration and were estimated to be accurate within the following limits for lift coefficients to at least 0.4:

C_L . . . . . ±0.005
C_{D_m} . . . . . ±0.001
C_m . . . . . ±0.001

The mass flow through the ducts and the internal drag were determined from pressure measurements made with a survey rake located at the model base. The internal-drag coefficients were estimated to be accurate within ±0.001. The base pressure for the ducts-closed condition was

determined from an orifice located inside the model base; the base pressure coefficient was estimated to be accurate within ±0.005.

The angle of attack was determined to within ±0.15° from a fixed-pendulum strain-gage unit located in the support sting and a calibration of sting and balance deflection with respect to model load.

Tests

All configurations were tested with the ducts open, and the basic configuration was also tested with the ducts closed.

The basic configuration and the configurations with leading-edge and chordwise fences were tested at Mach numbers from 0.6 to 1.12 at angles of attack up to 34°. At the higher Mach numbers, the maximum attainable angle of attack was reduced to 16° by tunnel power and balance limitations. Configurations with the vortex generators and chordwise extensions were tested at Mach numbers from 0.85 to 0.95 at angles of attack up to 20°. This limited Mach number and angle range was selected to cover the pitch-up region shown by the basic configuration.

Internal flow characteristics were measured for the configuration with the chordwise fences for angles of attack up to 15°. A tuft survey of the upper surface of the wing with and without chordwise fences was made at several Mach numbers and angles of attack in the pitch-up region.

The test Reynolds number based on the wing mean aerodynamic chord was of the order of 4.5×10^6 (fig. 5).

Corrections

The slotted walls of the test section minimize subsonic boundary interference effects, and no corrections for this interference have been applied.

The effects of supersonic boundary-reflected disturbances were reduced by testing the model a few inches off the tunnel center line. However, these disturbances caused the measured drag of the model at low lift coefficients to be too high at a Mach number of 1.05 and too low at a Mach number of 1.1. At Mach numbers above 1.1, the reflected disturbances were downstream of the model. The effects of the boundary-reflected disturbances have been minimized in the analysis plots by judicious fairing of the data plotted against Mach number. (See ref. 3.)

No corrections for sting interference have been applied. However, the effects on lift and pitching moment should be negligible (ref. 4),

whereas for drag they have been reduced for the ducts-closed case by base pressure adjustments and for the ducts-open case by using only the external drag in the analysis plots.

RESULTS

The results of this investigation are presented in the following figures:

	Figure
Miscellaneous data:	
Base pressures	6
Internal flow characteristics	7
Force and moment characteristics at constant Mach number:	
Basic configuration	8
Effects of chord-extensions	9
Effects of vortex generators	10
Effects of leading-edge fences	11
Effects of chordwise fences	12
Summary and analysis figures:	
Basic configuration	
Lift and pitch	13
Drag	14
Lift-drag ratios	15
Effects of fixes	
Lift and pitch	16
Drag	17
Lift-drag ratios	18
Flow studies:	
Tuft photographs	19
Schlieren photographs	20

All the drag data presented for the ducts-closed configuration have been adjusted to represent free-stream static pressure at the model base. The base pressure coefficients are presented in figure 6. The ducts-open drag data presented at constant Mach number in figures 8 to 12 include both external and internal drag. The ducts-open drag data presented in summary and analysis figures 14, 15, 17, and 18 have had the internal drag removed in order to present more realistic levels of drag at zero lift and maximum lift-drag ratio. The internal drag (fig. 7) was measured for the configuration with the chordwise fences only. However, the fixes should have no effect on internal flow and it was, therefore, assumed that the values of internal drag obtained were valid for the other configurations also. ?

It should be noted that the dark vertical lines at the left-hand edges of the schlieren photographs in figure 20(a) are not associated with the air flow over the model and have no significance for these tests.

In order to facilitate presentation of the data, staggered scales have been used in many of the figures and care should be taken in selecting the zero axis for each curve.

DISCUSSION

Lift Characteristics

Basic configuration.- The lift-curve slopes for the basic configuration with ducts open generally increased slightly with increasing angle of attack up to 10° for subsonic Mach numbers, whereas at supersonic speeds the lift curves were generally linear (fig. 8(a)). The average lift-curve slope varied from 0.044 to 0.053 (fig. 13).

At a Mach number of 0.8 (fig. 8(a)) the lift-curve slope decreased and approached zero at angles of attack from 10° to 12° ($C_L \approx 0.50$), but at higher angles approximately resumed its original value until effective maximum lift was reached. With increases in Mach number up to 0.95 the angle-of-attack range for the discontinuity or jog in the lift curve increased to 12° to 14° ($C_L \approx 0.63$). At Mach numbers above 0.95 the jog occurred at angles of attack above 16° ($C_L \approx 0.80$) or was no longer evident for the lift range tested. This discontinuity has been exhibited by other delta wings with thickness ratios from 2 to 6 percent (refs. 5 to 8, for example) and appeared to be associated with a loss of lift at the wing tips as the leading-edge separation vortex moved inboard (see fig. 19). The discontinuity at Mach numbers of 0.90 and 0.925 was probably accentuated by shock phenomena associated with wing-body interference.

A maximum lift coefficient of 0.91 was obtained at an angle of attack of 24° at a Mach number of 0.6. At Mach numbers from 0.80 to 0.925 effective maximum lift coefficients of 0.82 occurred at an angle of attack of 20°.

Effect of closing ducts.- The effects of closing the ducts on the lift characteristics of the basic configuration were minor (figs. 8(a) and 13).

Effect of wing fixes.- It will be shown in a subsequent section that in addition to the loss of lift-curve slope, the unloading of the wing tips at a lift coefficient of approximately 0.6 at high subsonic Mach numbers resulted in abrupt pitch-up. Since the pitch-up region would be entered in maneuvering flight at high altitudes several fixes were designed and tested in attempts to reduce or eliminate it.

Addition of chord-extensions beginning at the 60- or at the 70-percent-wing-semispan stations either substantially reduced or removed the discontinuity in the lift curves and increased the lift coefficients at angles of attack above 12° (fig. 9). The chord-extensions beginning at the 75- and 80-percent-semispan stations were generally ineffective and actually reduced the lift coefficient at which the jog occurred.

Except for a small increase in angle of attack and lift coefficient at which the jog occurred, neither of the two vortex-generator configurations was effective in improving the lift curves (fig. 10).

It was apparent from tests of the chord-extensions that the effective semispan location for the fences should be at or slightly inboard of the 70-percent station. On this basis, the 65-percent-wing-semispan station was chosen. Both the leading-edge and chordwise fences eliminated the discontinuity in the lift curves and generally increased the lift coefficients at angles of attack between 12° and at least 20° at subsonic Mach numbers (figs. 11(a) and 12(a)). The leading-edge fences also offered an increase of approximately 0.05 in effective maximum lift coefficient. Comparison of the tuft patterns for the wing with the chordwise fences on and off (fig. 19) indicated that a reduction in extent and severity of tip separation occurred when the fences were installed.

The effects of two of the successful fixes on the average lift-curve slope were small (fig. 16). Addition of the chord-extension from the 60-percent station increased the lift-curve slope by a percentage equal to the percentage increase in wing area.

Pitching-Moment Characteristics

Basic configuration.- The loss of lift at the wing tips which caused the decrease in lift-curve slope at a lift coefficient of approximately 0.6 for the basic configuration with the ducts open was accompanied by a forward shift in the center of pressure which resulted in a rapid increase in pitching moment, or pitch-up, at subsonic Mach numbers (fig. 8(c)). The discontinuity was particularly severe at Mach numbers of 0.90 and 0.925 where the pitching-moment coefficients increased approximately 0.02 with no increase in lift coefficient and then resumed the usual decrease with increasing lift coefficient.

The pitch-up may be effected by control deflections. Data not presented herein indicated that deflecting the elevons 15° trailing edge up on the basic configuration had no effect on the angle of attack at which the discontinuity occurred, but the magnitude of the abrupt increase in pitching moment was reduced by approximately 50 percent.

Except for the limited region near a lift coefficient of 0.6 at subsonic speeds, the configuration was stable through the test range. The value of the longitudinal stability parameter $\partial C_m/\partial C_L$ averaged over the linear portion of the curves varied from -0.08 at a Mach number of 0.6 to -0.17 at a Mach number of 1.1 (fig. 13), indicating a 9-percent $\bar{c}$ rearward shift in aerodynamic-center location.

Effect of closing ducts.- Closing the ducts of the basic configuration increased the severity of the pitch-up slightly at Mach numbers near 0.95 (fig. 8(c)) but had no effect on aerodynamic-center location (fig. 13).

Effect of wing fixes.- In evaluating the effects of wing fixes it should be noted that, although elimination of the jog or statically unstable variation of pitching-moment with angle of attack or lift greatly reduces the pitch-up, it does not necessarily indicate complete elimination of the pitch-up. Dynamic calculations (refs. 9 and 10) show that pitch-up can occur whenever the static margin is reduced from its initial value, or in different terms, whenever the pitch curve departs from linearity in the unstable direction. Also, rapid changes of pitching moment with Mach number can result in pitch-up even when the variations with angle of attack are linear.

The chord-extensions extending respectively from the 60- and 70-percent-wing-semispan stations to the tips reduced the pitch-up, with the 60-percent fix probably being the more favorable since it produced the generally more linear pitching-moment curves (fig. 9). The chord-extensions beginning outboard of the 70-percent station were ineffective and reduced the lift coefficient at which pitch-up occurred.

The vortex generators generally increased slightly the lift coefficient at which pitch-up occurred, but the pitch-up was not alleviated (fig. 10).

Addition of the leading-edge fences to the basic configuration resulted in large reductions in the original pitch-up (fig. 11(c)). However, a small region of neutral stability occurred at a lift coefficient of approximately 0.4 at Mach numbers of 0.90 and 0.925. The chordwise fences were effective in removing the discontinuity at a lift coefficient of 0.6 (fig. 12(c)), and more favorable stability characteristics were indicated for the region where the leading-edge-fence data had indicated neutral stability. Dynamic calculations (ref. 10) based on these data indicated that the chordwise fences removed about 90 percent of the pitch-up at a Mach number of 0.9.

In general, the data indicated that 0.25 chord-extensions beginning from the 60- to 70-percent-wing-semispan stations and leading-edge and chordwise fences located at the 65-percent-semispan station reduced the

pitch-up, whereas chord-extensions beginning outboard of the 70-percent-semispan station and the vortex-generator configurations tested were ineffective. Of the successful fixes tested, the chord-extension beginning at the 60-percent-semispan station and the chordwise fences were probably the most favorable. As compared with the plain wing, addition of the chordwise fences had no effect on the longitudinal stability parameter averaged over the low-lift linear portion of the curve, whereas the chord-extension beginning at the 60-percent-semispan station moved the center of pressure forward and resulted in a 2-percent $\bar{c}$ forward shift in the aerodynamic-center location (fig. 16).

Drag Characteristics

Basic configuration.- The drag polars presented for the basic configuration with ducts open in figure 8(b) indicated that the minimum drag occurred at approximately zero lift. As would be expected, abrupt increases in drag with increasing lift were indicated at a lift coefficient of approximately 0.6 at high subsonic Mach numbers. These increases were the result of the tip separation which caused the discontinuities previously shown in the lift and pitch curves.

The zero-lift drag rise began at a Mach number of approximately 0.91 and peaked at a Mach number of about 1.05 (fig. 14). The rather large magnitude of the drag rise (0.02) was probably due to the unfavorable cross-sectional area distribution for the model. It has been shown (ref. 11, for example) that the zero-lift drag rise for wing-body combinations near the speed of sound is a function of the rate of axial development of total cross-sectional area of the model. It can be seen in figure 3 that the canopy and ducts are located in the same axial position and therefore cause an abrupt increase in area at that point. More importantly, however, the wing and vertical tail are located near the after end of the configuration and result in a very rapid decrease in cross-sectional area from the point of maximum area to the model base. Rapid changes in cross-sectional area, especially decreases in area, are conducive to large drag rises. The schlieren photographs of figure 20(b) indicated the presence of strong shock waves at transonic Mach numbers just forward of the model base in the region of rapidly decreasing cross-sectional area.

The values of drag-due-to-lift factor $\frac{dC_D}{dC_L^2}$ for the basic configuration were high, ranging from 0.32 at a Mach number of 0.6 to 0.28 at Mach numbers above 1.05 (fig. 14). The curves in figure 14 for no leading-edge suction were obtained by assuming the drag due to lift to be equal to $C_L \tan \alpha$, and the theoretical full leading-edge suction values were calculated from references 12 and 13. It will be noted that approximately 35 percent full leading-edge suction was obtained through the Mach number range. Increases in Reynolds number to full-scale values

should increase the leading-edge suction and reduce the drag due to lift at Mach numbers below about 0.90. At higher Mach numbers, however, little benefit can be expected from increases in Reynolds number (see ref. 14).

The maximum lift-drag ratio for the basic configuration was approximately 9.5 at subcritical Mach numbers and decreased to 5.5 at Mach numbers above 1.0 (fig. 15). The maximum lift-drag ratio occurred at lift coefficients varying from 0.17 at a Mach number of 0.60 to 0.30 at Mach numbers above 1.025 (fig. 15).

Effect of closing ducts.- Closing the ducts of the basic configuration had no effect on drag-rise Mach number and magnitude of the drag rise at zero lift (fig. 14). Except for Mach numbers from 0.95 to 1.05, closing the ducts decreased the drag due to lift slightly (fig. 14). The maximum lift-drag ratios and lift coefficient for maximum lift-drag ratio were not significantly affected by closing the ducts (fig. 15).

Effect of wing fixes.- Addition of chord-extensions from the 60- and 70-percent-wing-semispan stations generally eliminated the jog in the drag polars (fig. 9) and resulted in lower drag coefficients at lift coefficients above approximately 0.6. Chord-extensions beginning outboard of the 70-percent station had no beneficial effect.

Vortex generators had no beneficial effect on the drag polars (fig. 10), whereas the leading-edge and chordwise fences eliminated the jog (figs. 11(b) and 12(b)).

At zero lift the drag level at Mach numbers above 1.03 was reduced slightly by addition of the chordwise fences (fig. 17). Because of the added area, the drag level for the chord-extension case was slightly higher than for the basic configuration. The chord-extensions had little effect on drag due to lift (fig. 17); however, the chordwise fences reduced the drag-due-to-lift factor by approximately 16 percent at Mach numbers from 0.6 to 0.95. At higher Mach numbers, the beneficial effects decreased and, at a Mach number of 2.0, data presented in reference 1 indicated that fences had no effect on the drag due to lift. The chordwise fences resulted in significant increases in maximum lift-drag ratio (fig. 18). The wing fixes had little effect on the lift coefficient for maximum lift-drag ratio (fig. 18).

It was previously shown that the chordwise fences and the chordwise extension beginning at the 60-percent-semispan station were the most successful fixes with regard to the pitch-up problem. Since the chordwise fences offer substantial reductions in drag at lifting conditions while the chord-extensions do not, it may be concluded that the chordwise fences are the most satisfactory fix for this configuration.

CONCLUSIONS

The following may be concluded from wind-tunnel tests of a 1/20-scale model of the Convair F-102 airplane at transonic speeds:

1. The basic configuration exhibited a serious pitch-up phenomenon at a lift coefficient of approximately 0.6 at high subsonic Mach numbers. The phenomenon was also reflected in unfavorable lift and drag characteristics in the same lift-coefficient and Mach number ranges.

2. The pitch-up and its attendant effects on the lift and drag characteristics were generally reduced by wing fixes including chord-extensions beginning at the 60- or 70-percent-wing-semispan stations, and by leading-edge or chordwise fences at the 65-percent-semispan station. Chord-extensions beginning outboard of the 70-percent-wing-semispan station and vortex generators were ineffective in reducing pitch-up.

3. The magnitude of the drag rise at zero lift and the drag due to lift were high; the maximum lift-drag ratios were approximately 9.5 at subcritical speeds and 5.5 at Mach numbers above 1.0.

4. The chordwise fences were the most satisfactory fix for the airplane since they reduced the pitch-up and in addition decreased the drag due to lift.

Langley Aeronautical Laboratory,
National Advisory Committee for Aeronautics,
Langley Field, Va., March 5, 1954.

Robert S. Osborne
Robert S. Osborne
Aeronautical Research Scientist

Dewey E. Wornom
Dewey E. Wornom
Aeronautical Research Scientist

Approved: Eugene C. Draley
Eugene C. Draley
Chief of Full Scale Research Division

DY

REFERENCES

1. Hilton, John H., Jr., Hamilton, Clyde V., and Lankford, John L.: Preliminary Wind-Tunnel Investigation of a 1/20-Scale Model of the Convair MX-1554 at Mach Numbers of 1.61 and 2.01. NACA RM SL52L11a, U. S. Air Force, 1952.

2. Ritchie, Virgil S., and Pearson, Albin O.: Calibration of the Slotted Test Section of the Langley 8-Foot Transonic Tunnel and Preliminary Experimental Investigation of Boundary-Reflected Disturbances. NACA RM L51K14, 1952.

3. Osborne, Robert S., and Mugler, John P., Jr.: Aerodynamic Characteristics of a 45° Sweptback Wing-Fuselage Combination and the Fuselage Alone Obtained in the Langley 8-Foot Transonic Tunnel. NACA RM L52E14, 1952.

4. Osborne, Robert S.: High-Speed Wind-Tunnel Investigation of the Longitudinal Stability and Control Characteristics of a 1/16-Scale Model of the D-558-2 Research Airplane at High Subsonic Mach Numbers and at a Mach Number of 1.2. NACA RM L9C04, 1949.

5. Kelly, Thomas C.: Transonic Wind-Tunnel Investigation of the Aerodynamic Characteristics of a 60° Triangular Wing in Combination with a Systematic Series of Three Bodies. NACA RM L52L22a, 1953.

6. Palmer, William E.: Effect of Reduction in Thickness From 6 to 2 Percent and Removal of the Pointed Tips on the Subsonic Static Longitudinal Stability Characteristics of a 60° Triangular Wing in Combination With a Fuselage. NACA RM L53F24, 1953.

7. Wiggins, James W.: Wind-Tunnel Investigation at High Subsonic Speeds of the Static Longitudinal and Static Lateral Stability Characteristics of a Wing-Fuselage Combination Having a Triangular Wing of Aspect Ratio 2.31 and an NACA 65A003 Airfoil. NACA RM L53G09a, 1953.

8. Smith, Donald W., and Heitmeyer, John C.: Lift, Drag, and Pitching Moment of Low-Aspect-Ratio Wings at Subsonic and Supersonic Speeds - Plane Triangular Wing of Aspect Ratio 2 With NACA 0005-63 Section. NACA RM A50K21, 1951.

9. Campbell, George S., and Weil, Joseph: The Interpretation of Nonlinear Pitching Moments in Relation to the Pitch-Up Problem. NACA RM L53I02, 1953. NASA TN D-193

10. Roderick, H.: Investigation of Pitch Up Effects on the F-102 Airplane. Dynamics Memo DC-8-134 (Contract #AF33(600)-5942), Consolidated Vultee Aircraft Corp., July 30, 1953.

11. Whitcomb, Richard T.: A Study of the Zero-Lift Drag-Rise Characteristics of Wing-Body Combinations Near the Speed of Sound. NACA RM L52H08, 1952.

12. Jones, Robert T.: Estimated Lift-Drag Ratios at Supersonic Speed. NACA TN 1350, 1947.

13. DeYoung, John: Theoretical Additional Span Loading Characteristics of Wings With Arbitrary Sweep, Aspect Ratio, and Taper Ratio. NACA TN 1491, 1947.

14. Osborne, Robert S., and Kelly, Thomas C.: A Note on the Drag Due to Lift of Delta Wings at Mach Numbers up to 2.0. NACA RM L53A16a, 1953.

TABLE I

DIMENSIONS OF THE 1/20-SCALE MODEL OF THE CONVAIR F-102 AIRPLANE

Basic wing:	
Airfoil section	NACA 0004-~~64~~ 65 (mod.)
Total area, sq ft	1.625
Aspect ratio	2.2
Taper ratio	0
Incidence, deg	0
Dihedral, deg	0
Longitudinal location of center of gravity, percent $\bar{c}$	27.5
Vertical location of center of gravity above wing chord plane, percent $\bar{c}$	3.6
Fuselage:	
Frontal area (without canopy), sq ft	0.075
Fineness ratio (without canopy)	7.9
Base area (including sting), sq ft	0.0345
Projected inlet area at $\alpha = 0^{\circ}$, sq ft	0.0099
Duct exit area (excluding sting), sq ft	0.0179
Vertical tail:	
Airfoil section	NACA 0004-65 (mod.)
Exposed area, sq ft	0.1704
Aspect ratio	1.1
Taper ratio	0
Equivalent body of revolution:	
Maximum diameter (including inlet area), in.	4.64
Fineness ratio (including inlet area)	6.3
Maximum diameter (inlet area removed), in.	4.47
Fineness ratio (inlet area removed)	6.6

TABLE II

ORDINATES OF THE NACA 0004-65 (MODIFIED) AIRFOIL SECTION AS USED ON THE 1/20-SCALE MODEL OF THE CONVAIR F-102 AIRPLANE

Station, percent c	Ordinate, percent c
0	0
.25	.28
.50	.39
.75	.47
1.00	.53
1.25	.59
2.50	.79
5.00	1.03
7.50	1.20
10.00	1.32
20.00	1.64
30.00	1.83
40.00	1.95
50.00	2.00
60.00	1.97
70.00	1.82
80.00	1.40
90.00	.73
100.00	----
Leading-edge radius: 0.0018c	

L-76485.1

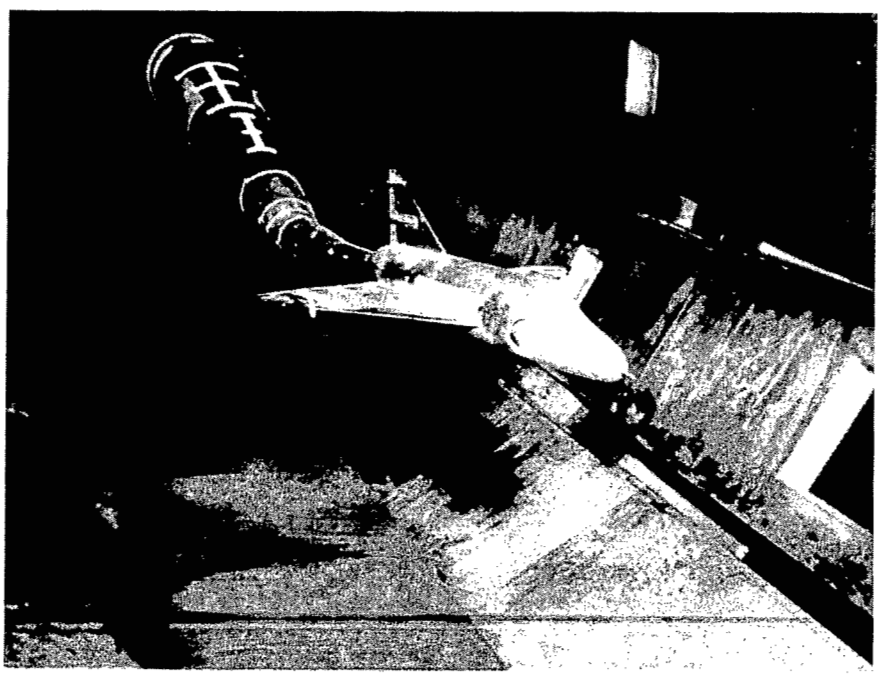

L-76486.1

Figure 1.- Photographs of the 1/20-scale model of the Convair F-102 airplane with leading-edge fences and open ducts as tested in the Langley 8-foot transonic tunnel.

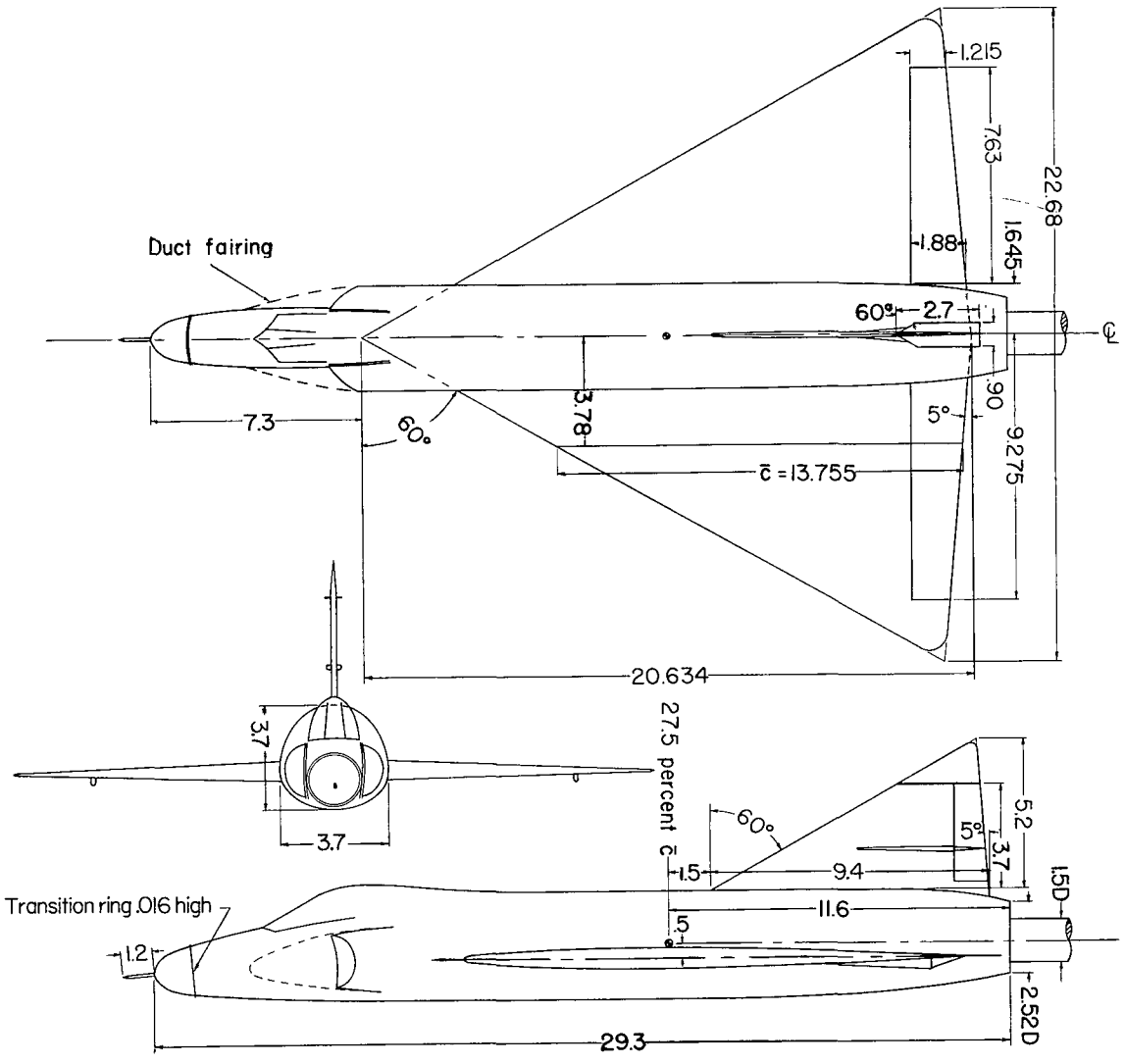

Figure 2.- Model details. All dimensions are in inches unless otherwise noted.

[redacted]

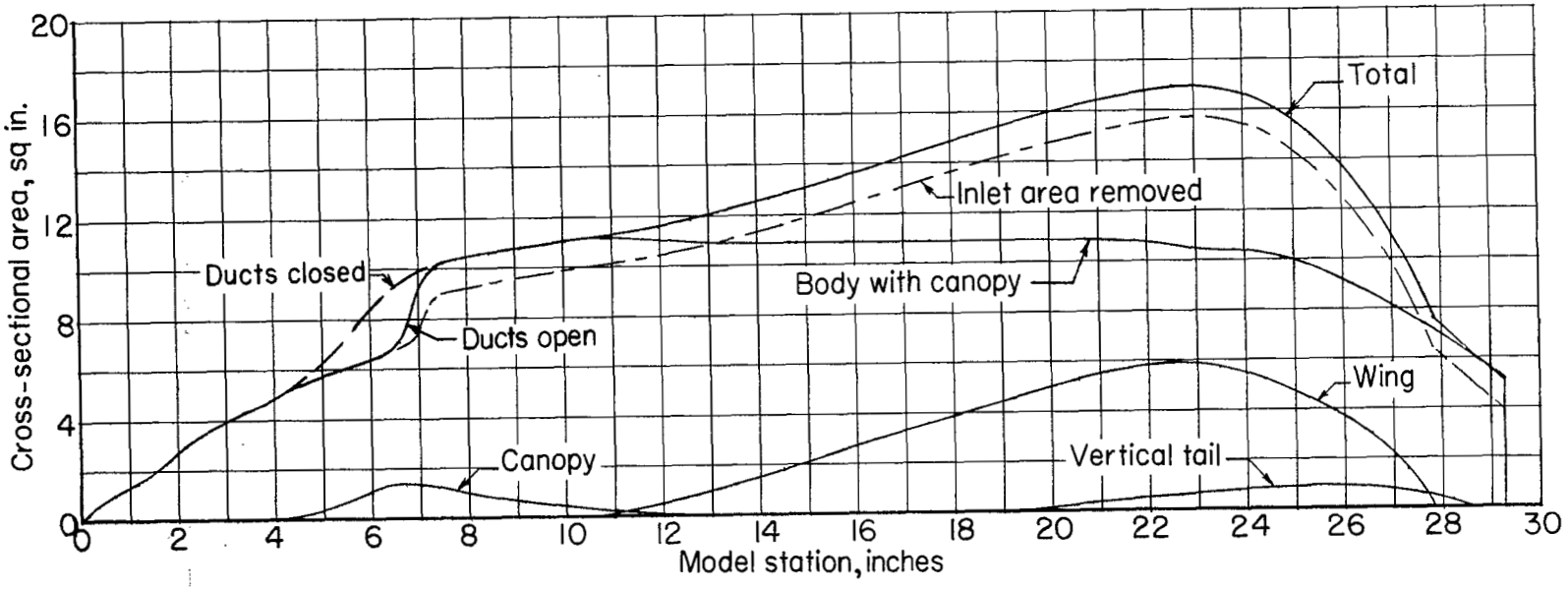

Figure 3.- Axial distribution of cross-sectional area of the basic configuration with ducts open and closed.

[redacted]

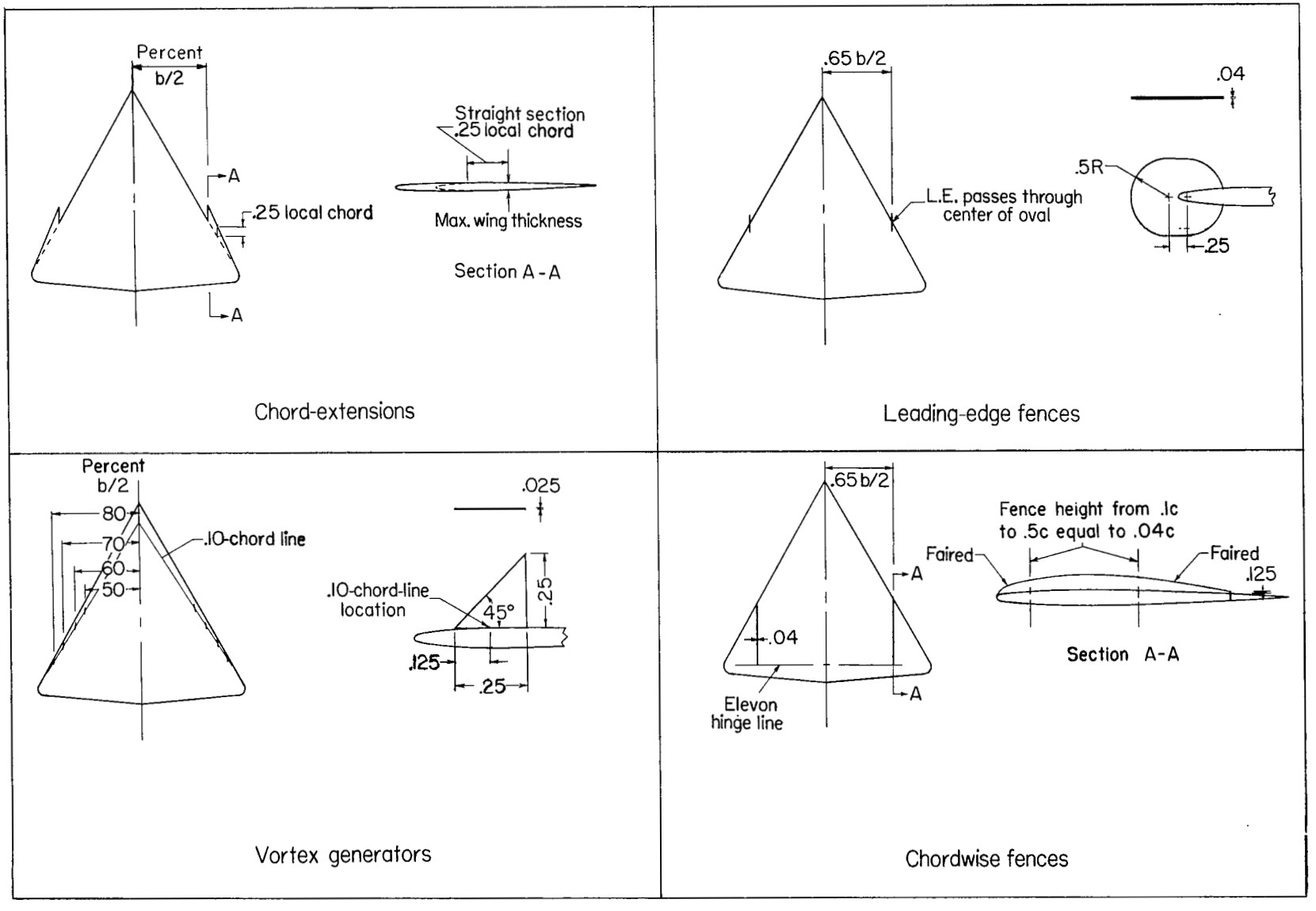

Figure 4.- Dimensional details and location of wing fixes. All dimensions are in inches unless otherwise noted.

[redacted]

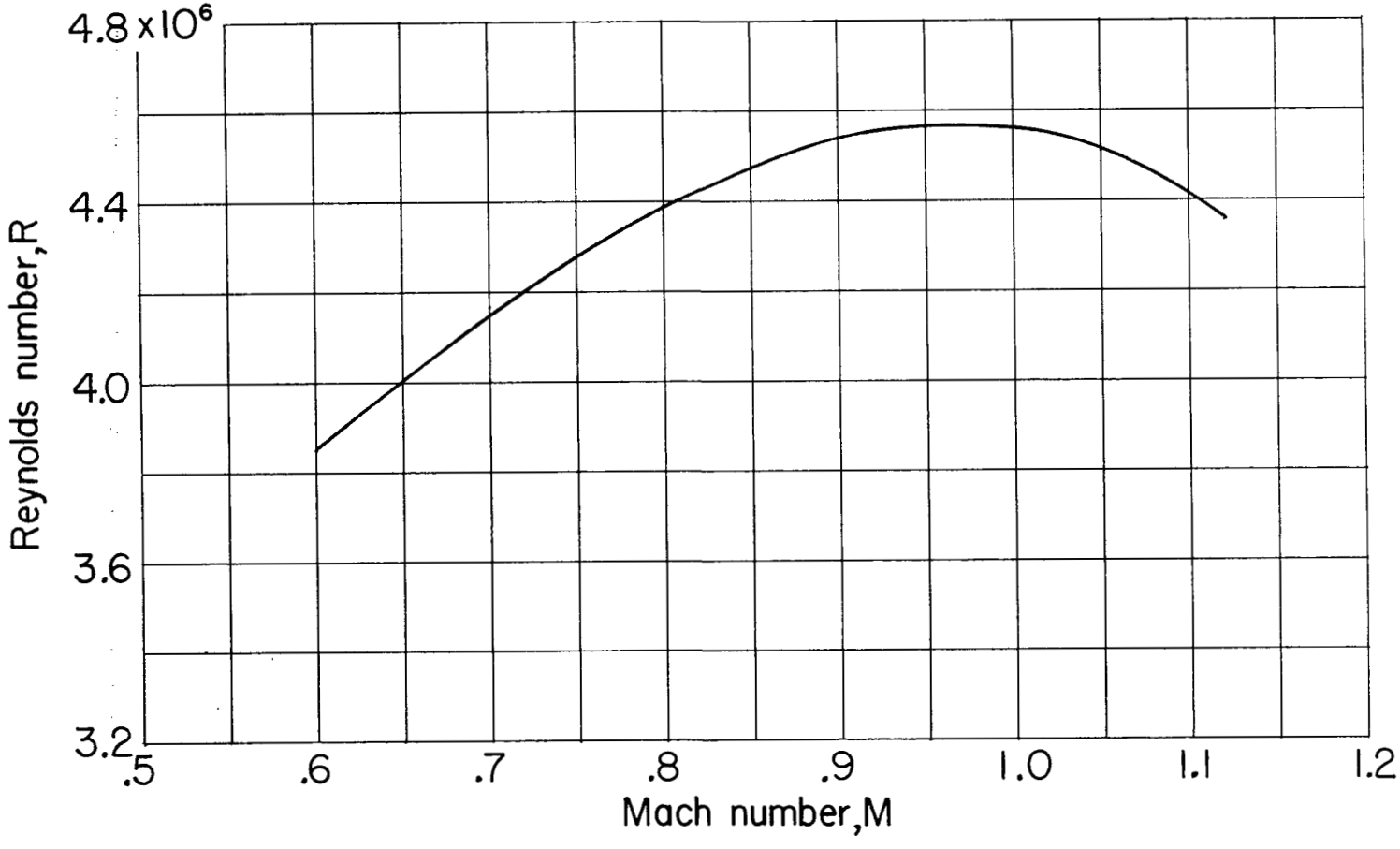

Figure 5.- Variation with Mach number of approximate test Reynolds number based on $\bar{c}$ = 13.755 inches.

[redacted]

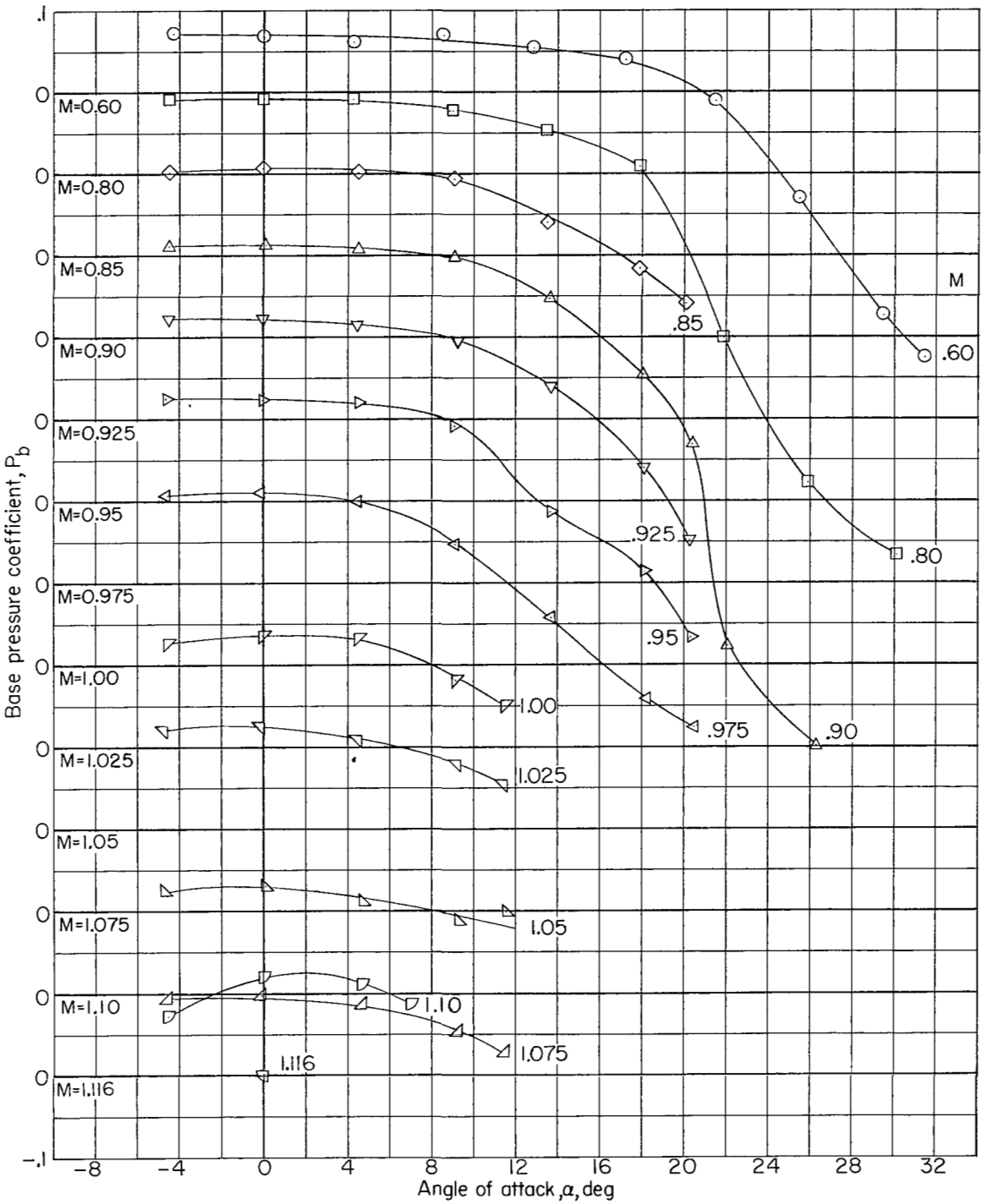

Figure 6.- Base-pressure coefficients for the basic configuration with ducts closed.

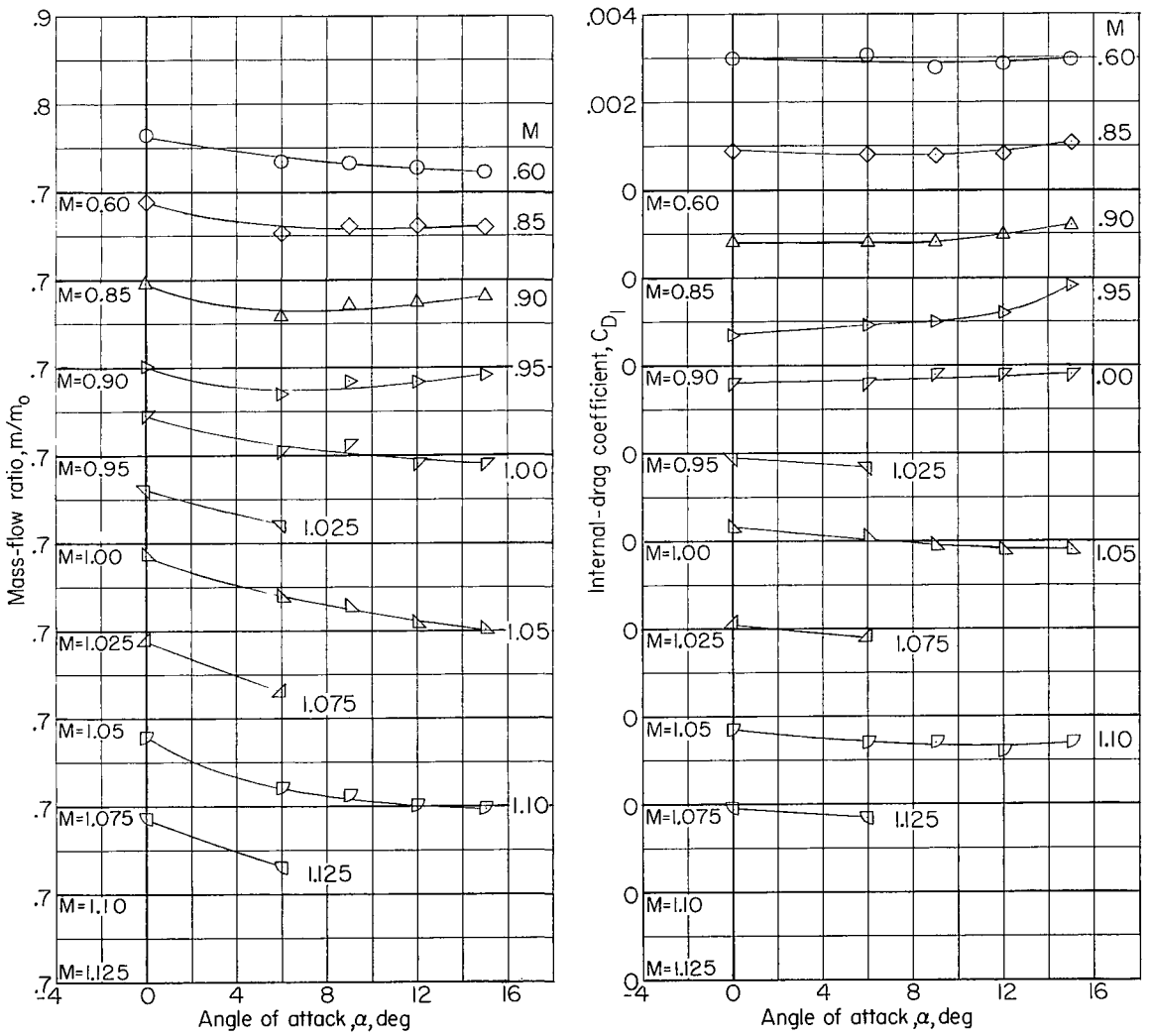

Figure 7.- Mass-flow ratios and internal drag coefficients for the basic configuration with chordwise fences. Ducts open.

[redacted]

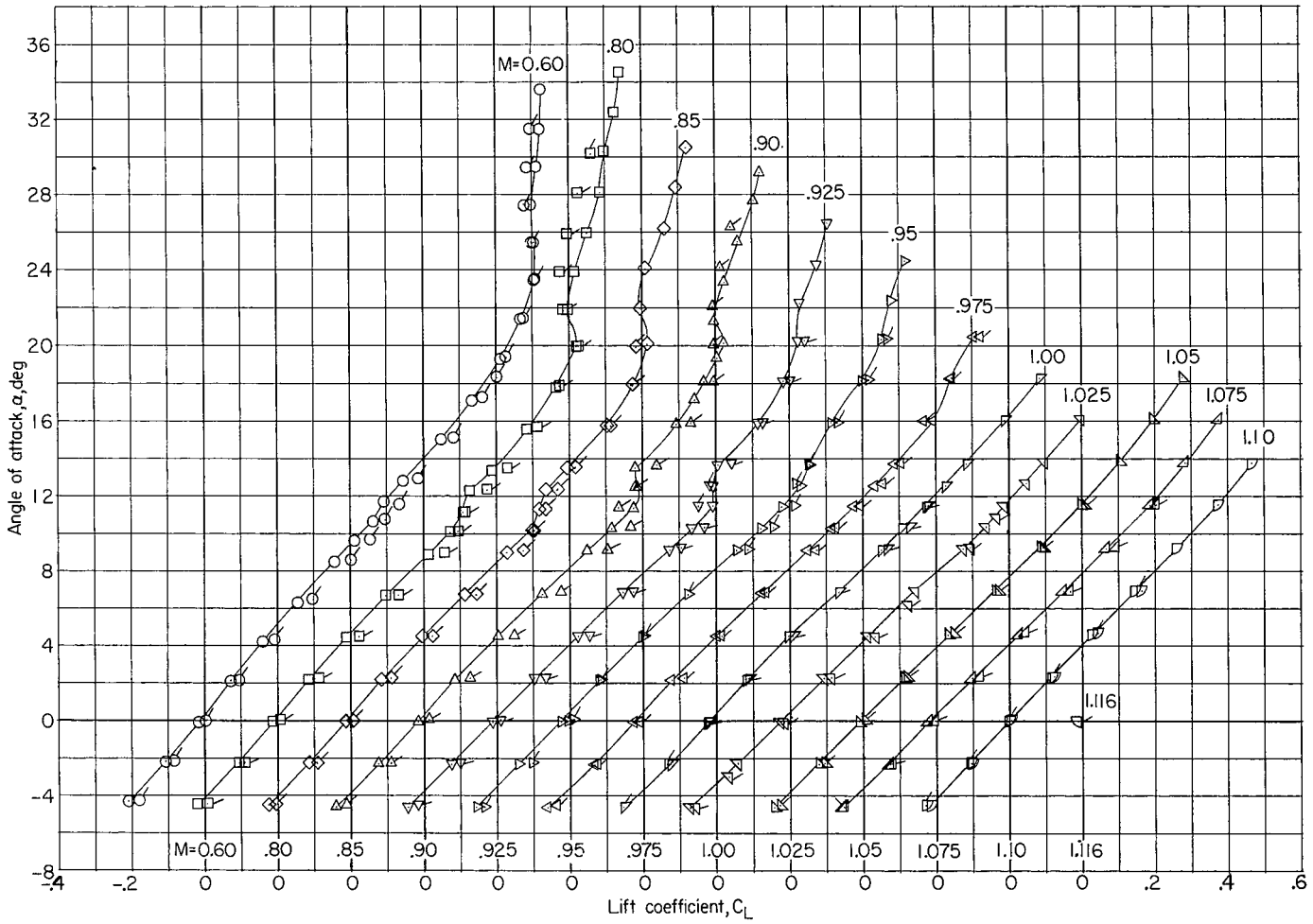

(a) Lift.

Figure 8.- Force and moment characteristics of the basic configuration with ducts open and closed. Ducts-open data include internal drag. Flagged symbols indicate ducts closed.

[redacted]

[redacted]

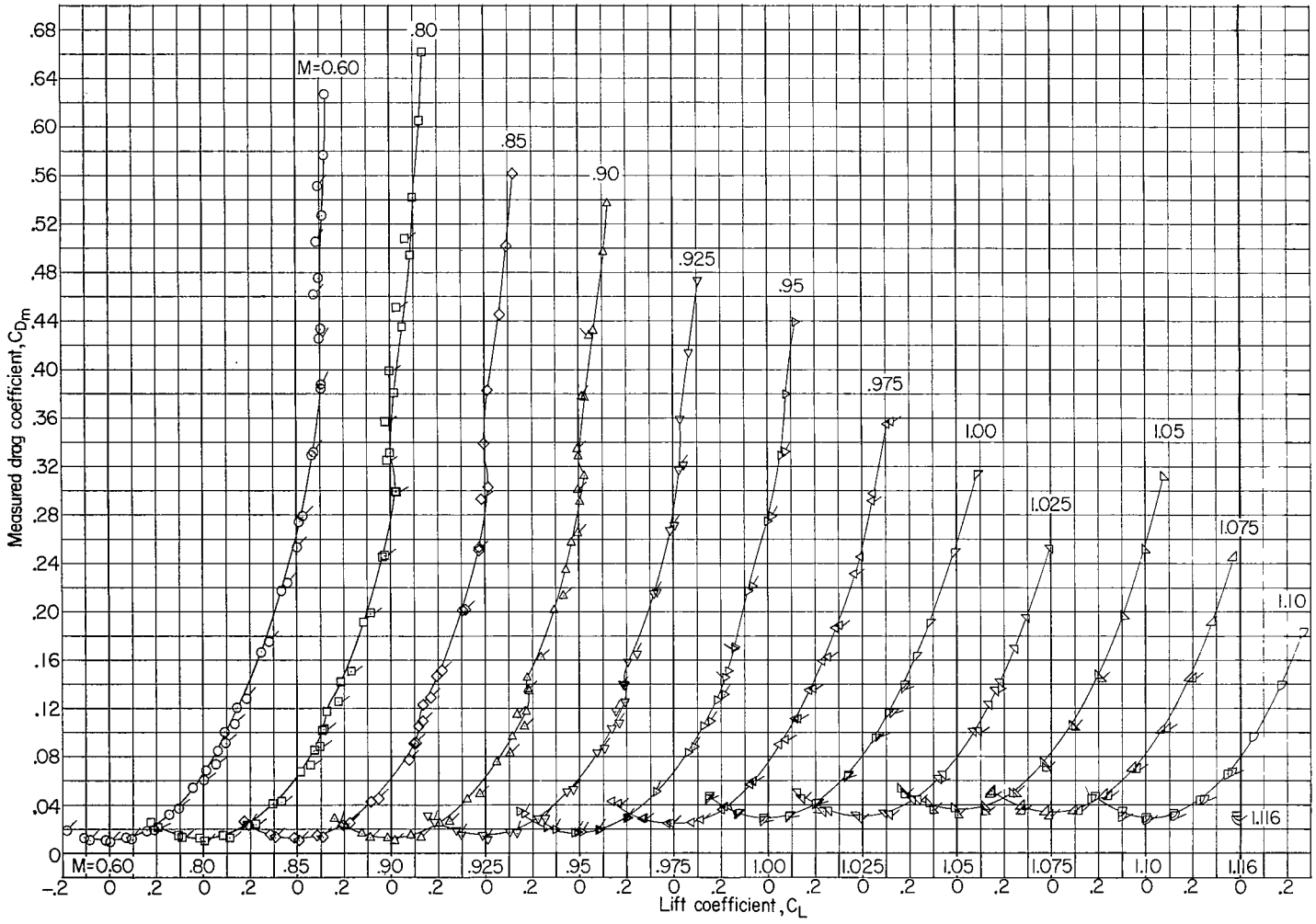

(b) Drag.

Figure 8.- Continued.

[redacted]

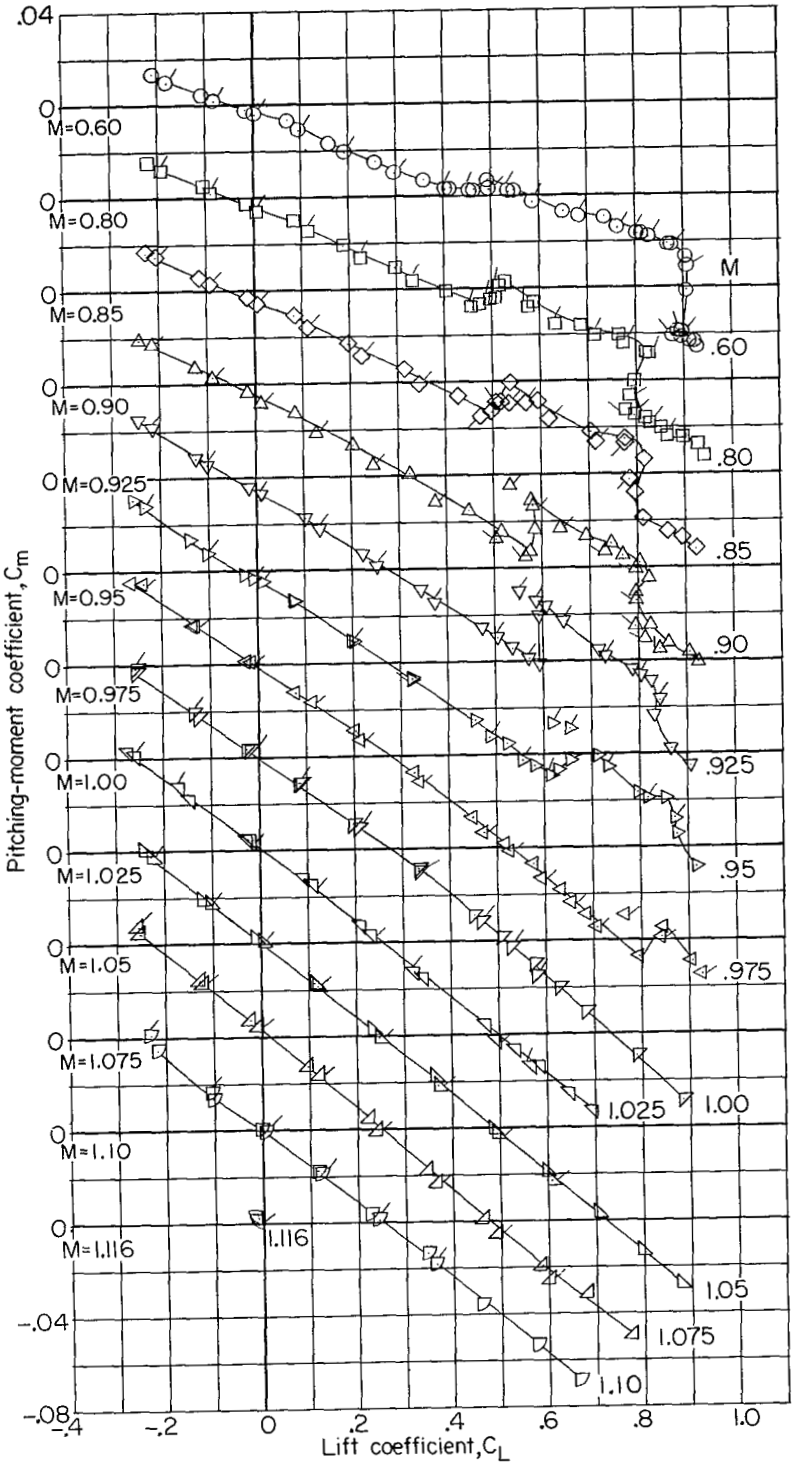

(c) Pitching moment.

Figure 8.- Concluded.

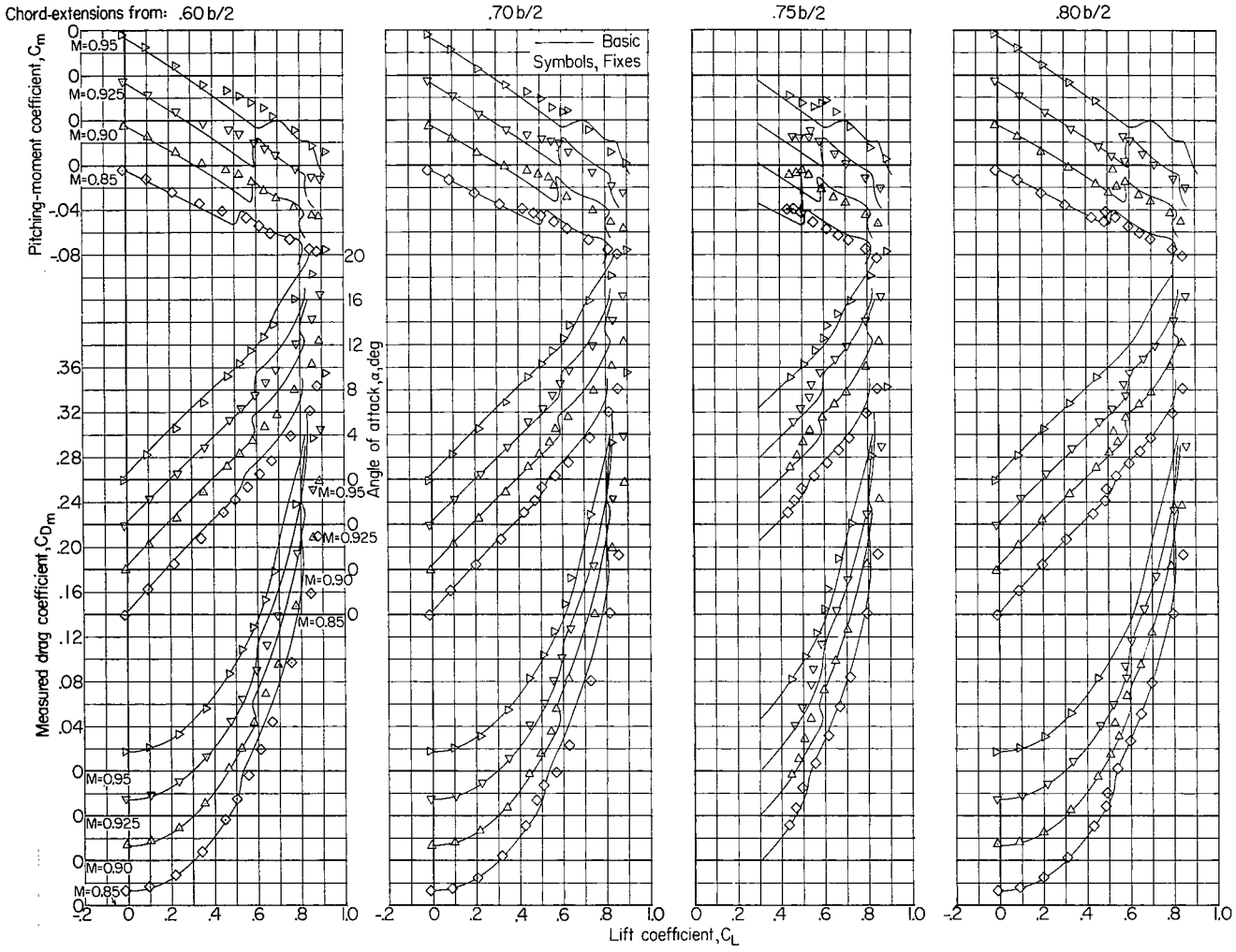

Figure 9.- Effect of chord-extensions on the force and moment characteristics of the basic configuration with ducts open. Internal drag included. Solid lines are basic configuration; symbols indicate fix.

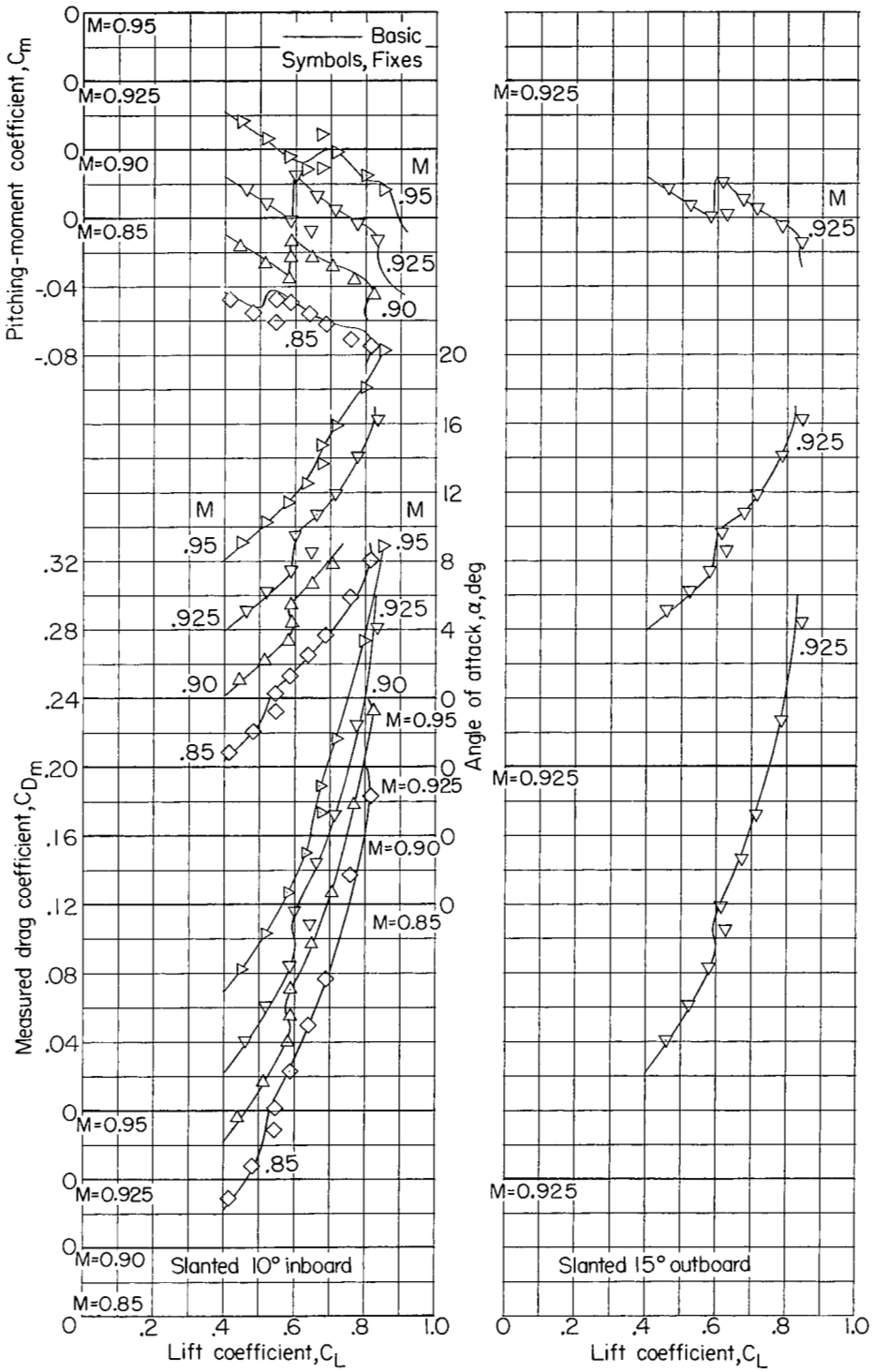

Figure 10.- Effect of vortex generators on the force and moment characteristics of the basic configuration with ducts open. Internal drag included. Solid lines are basic configuration; symbols indicate fix.

[redacted]

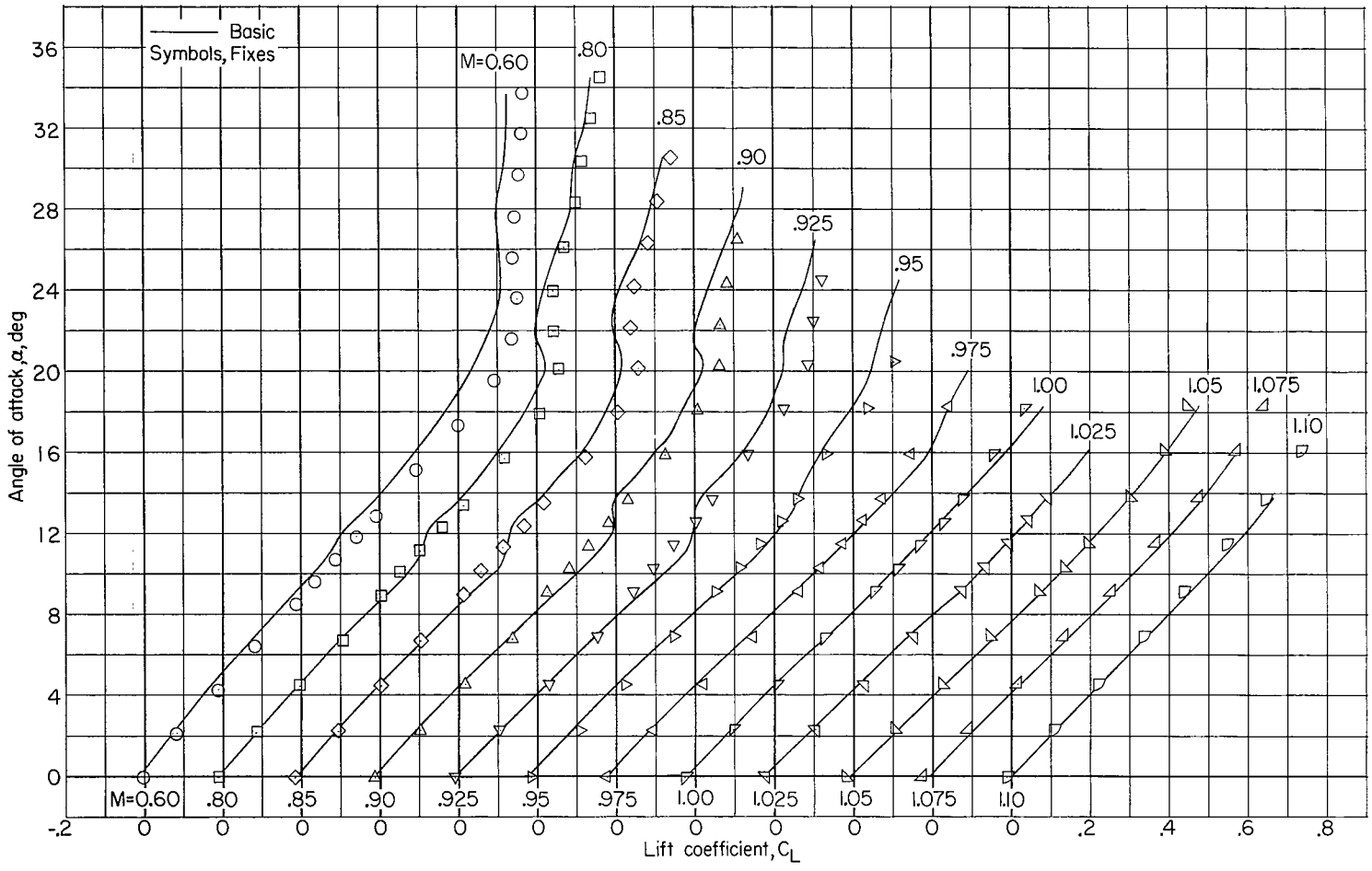

(a) Lift.

Figure 11.- Effect of leading-edge fences on the force and moment characteristics of the basic configuration with ducts open. Internal drag included. Solid lines represent basic configuration; symbols indicate fix.

[redacted]

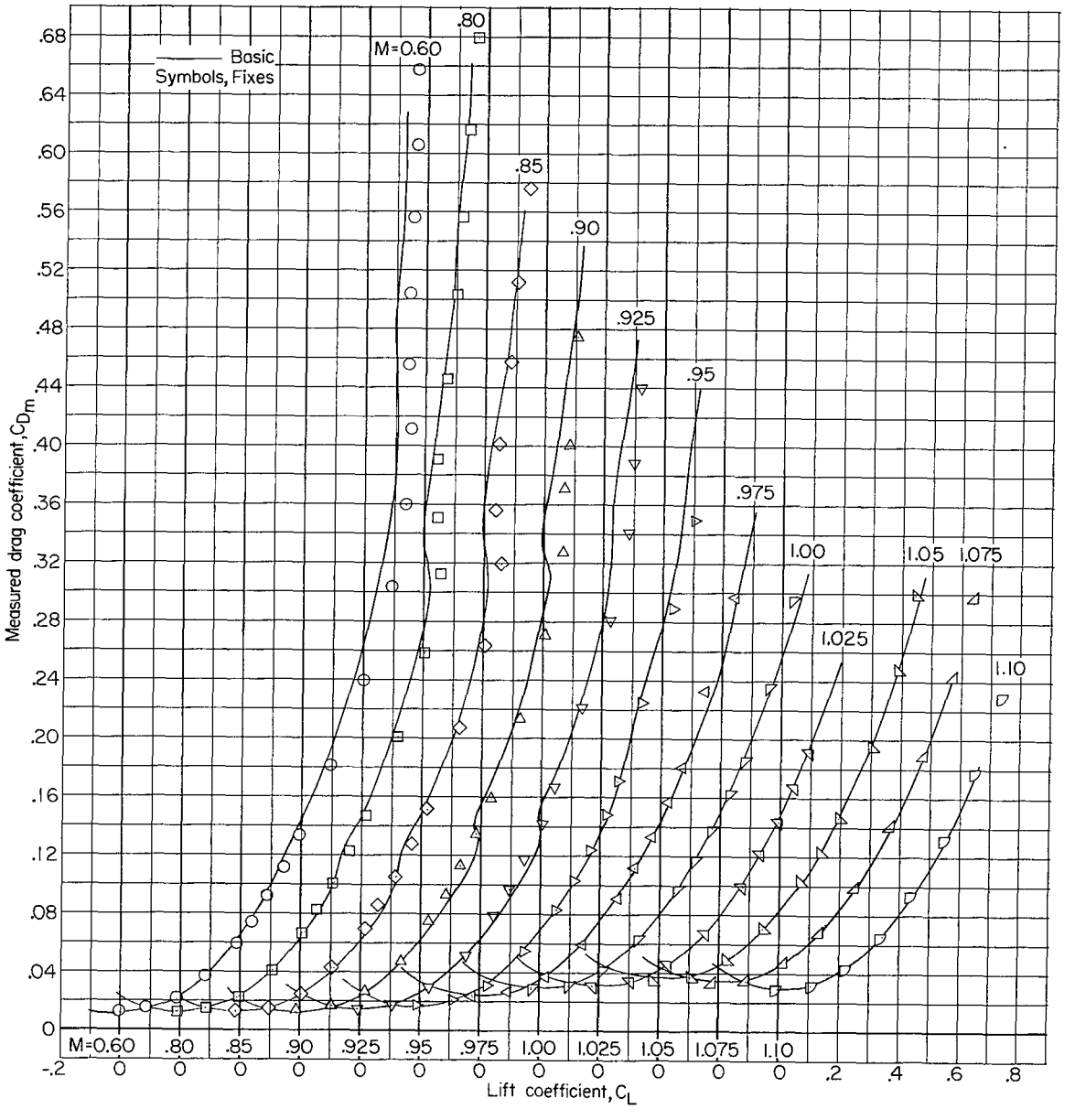

(b) Drag.

Figure 11.- Continued.

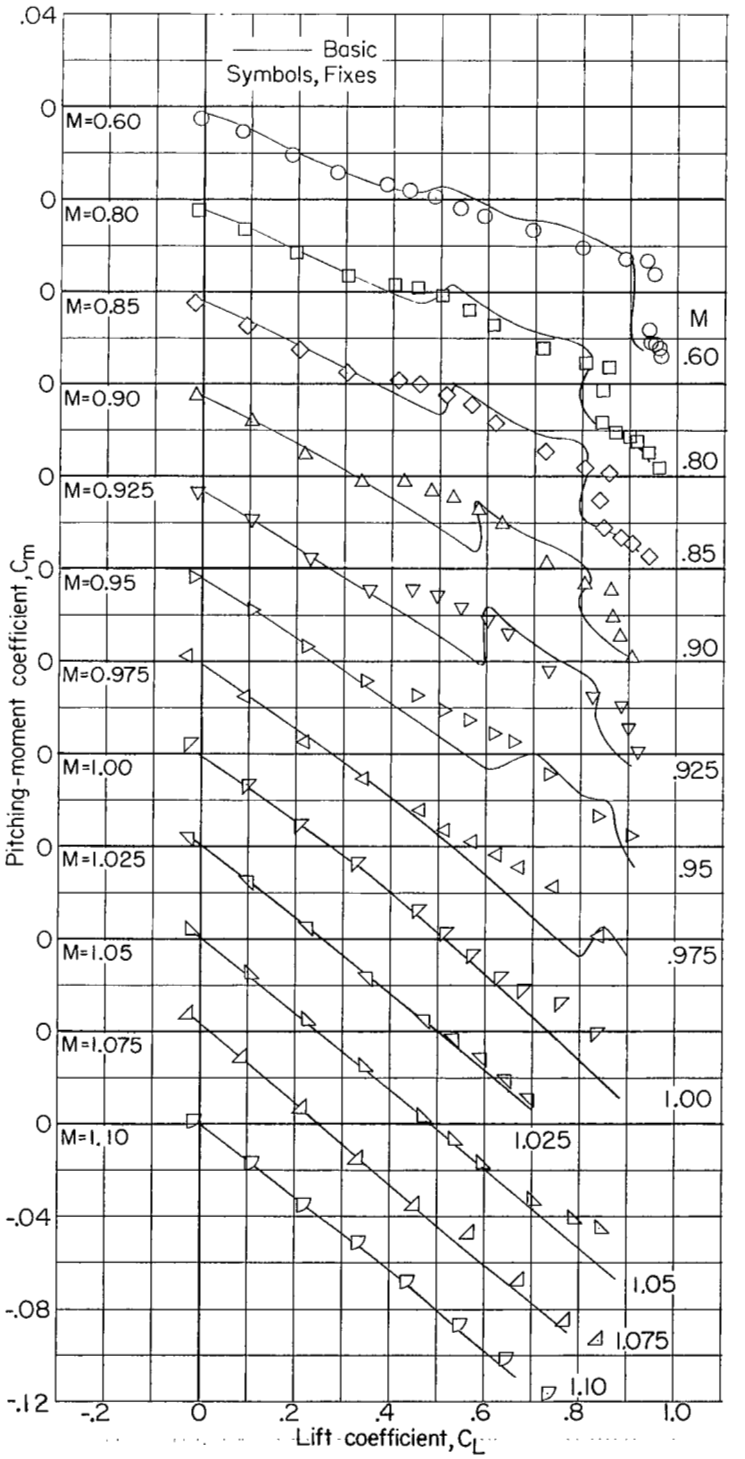

(c) Pitching moment.

Figure 11.- Concluded.

[redacted]

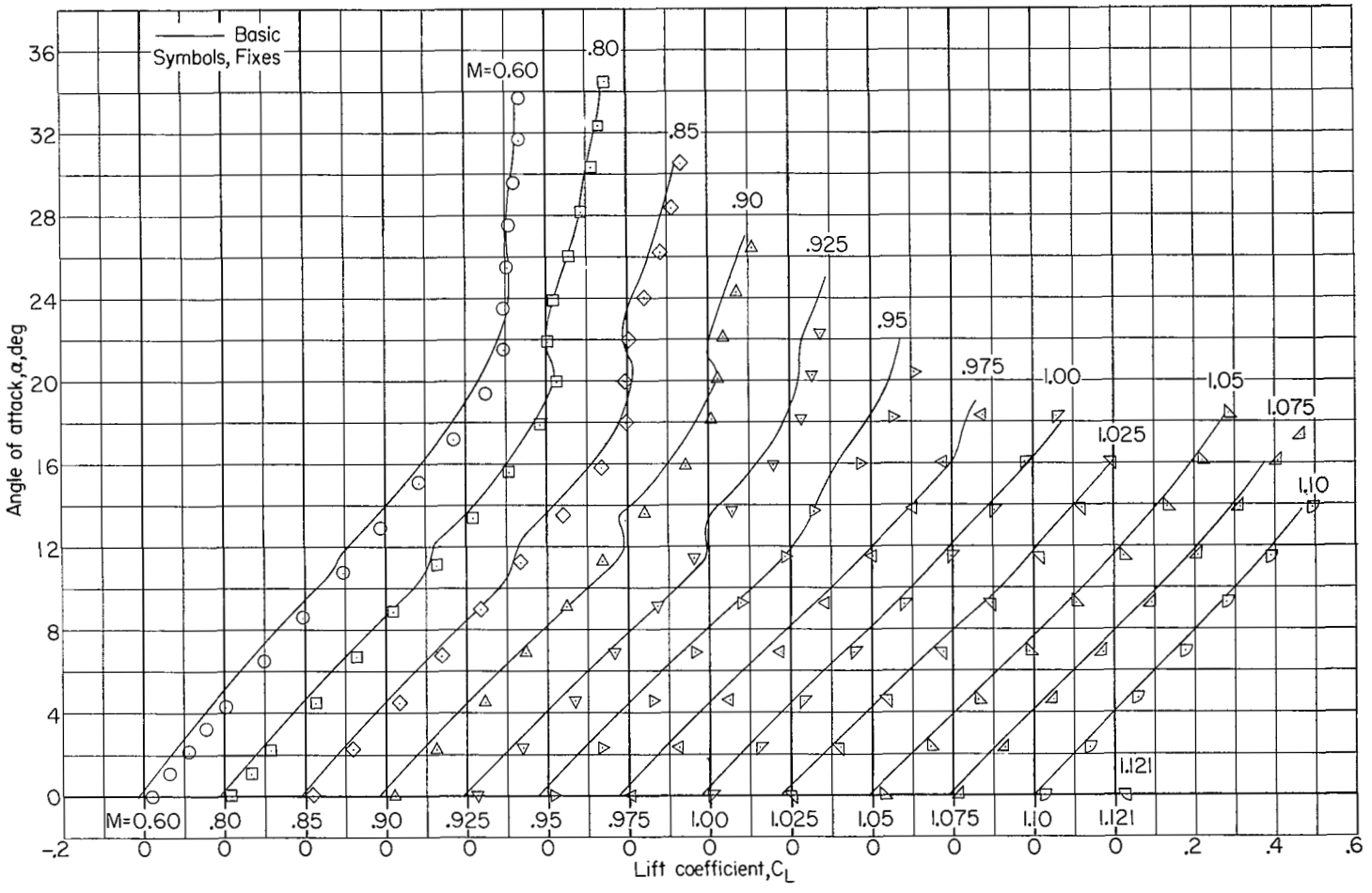

(a) Lift.

Figure 12.- Effect of chordwise fences on the force and moment characteristics of the basic configuration with ducts open. Internal drag included. Solid lines represent basic configuration; symbols indicate fix.

[redacted]

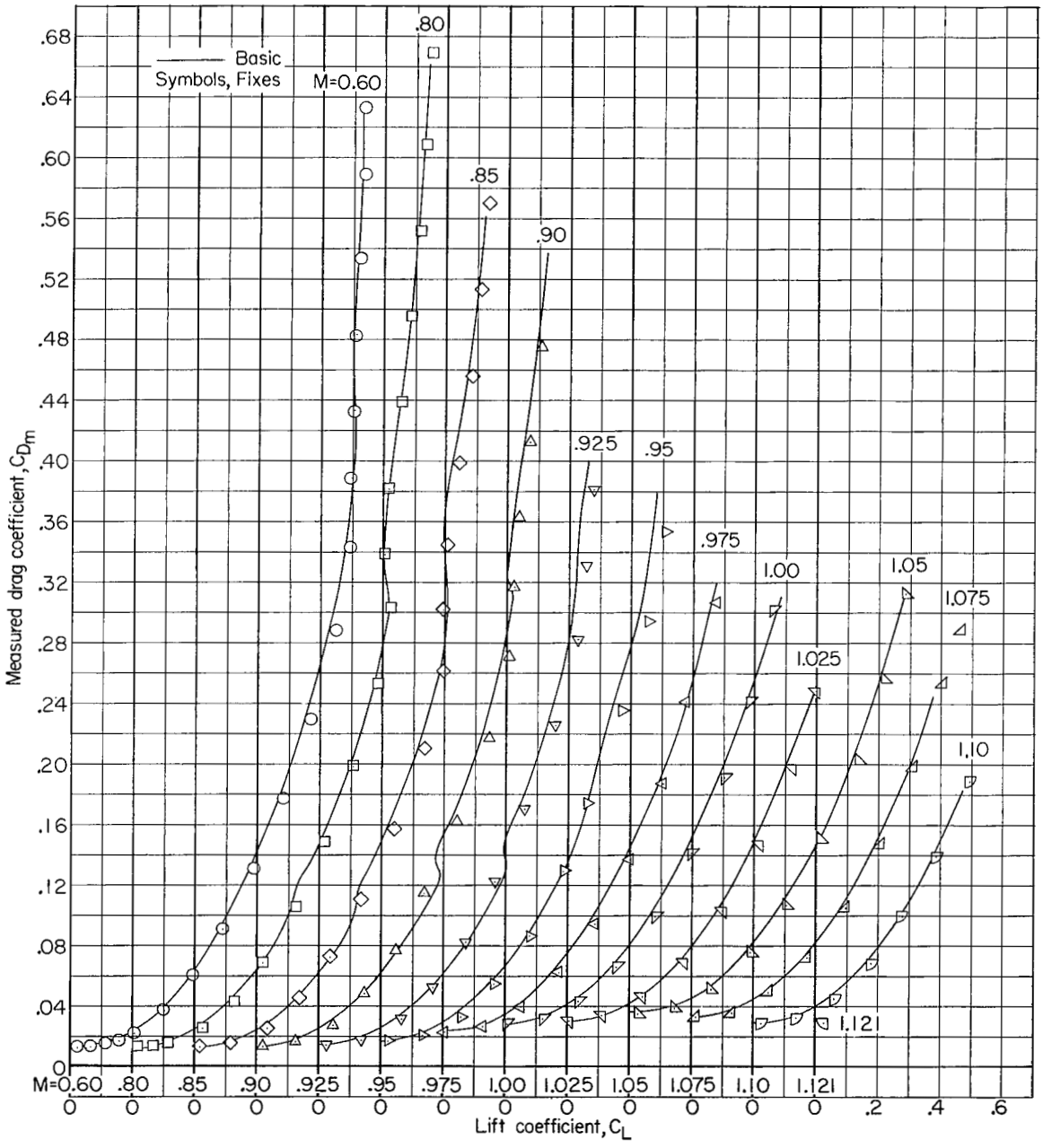

(b) Drag.

Figure 12.- Continued.

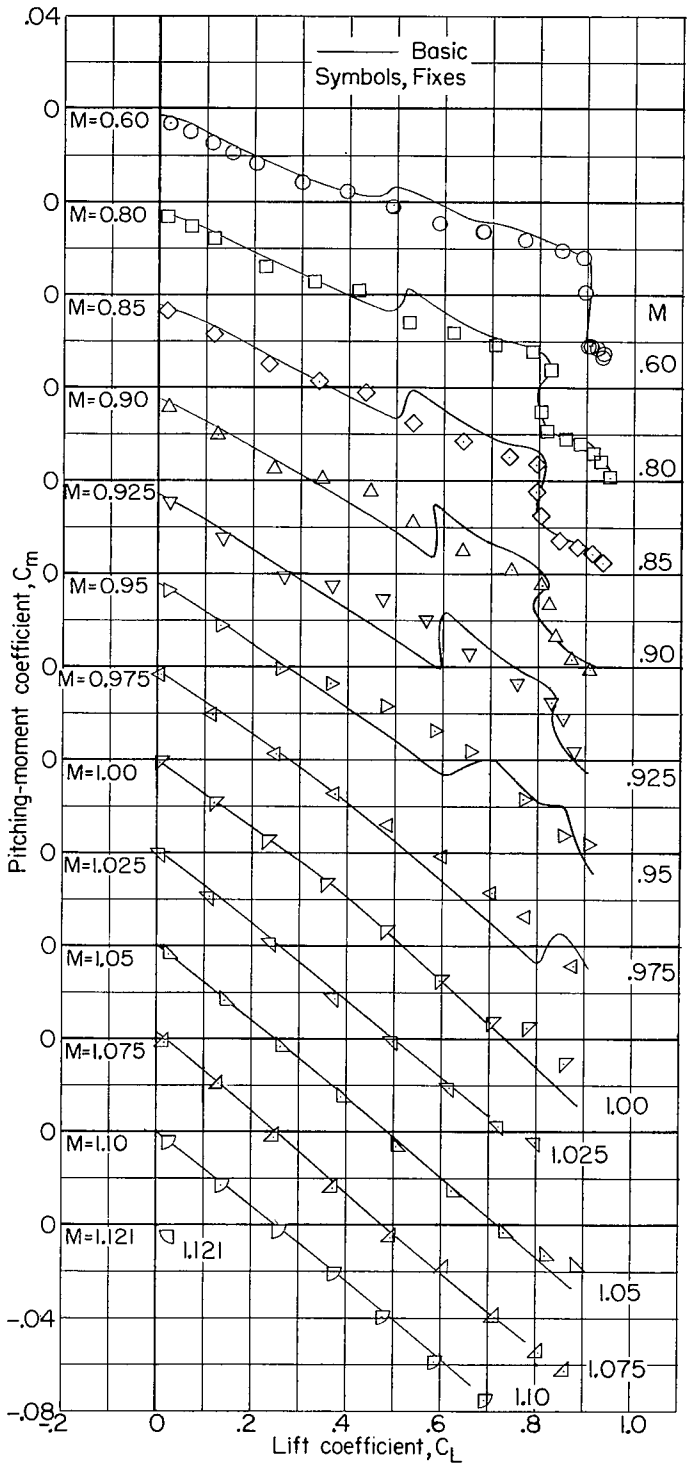

(c) Pitching moment.

Figure 12.- Concluded.

[redacted]

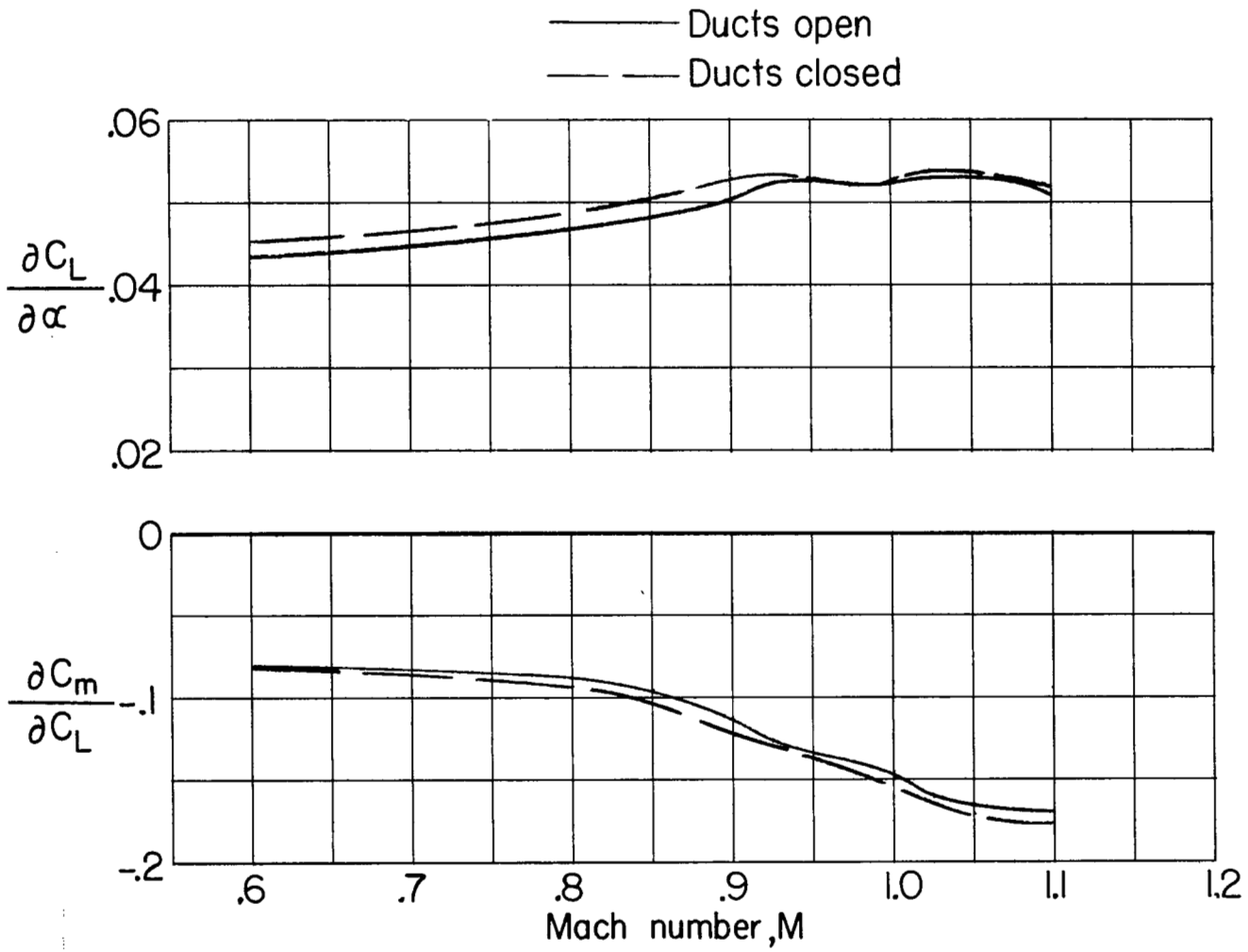

Figure 13.- Variation with Mach number of the average lift-curve slope and static-longitudinal-stability parameter for the basic configuration with ducts open and closed.

[redacted]

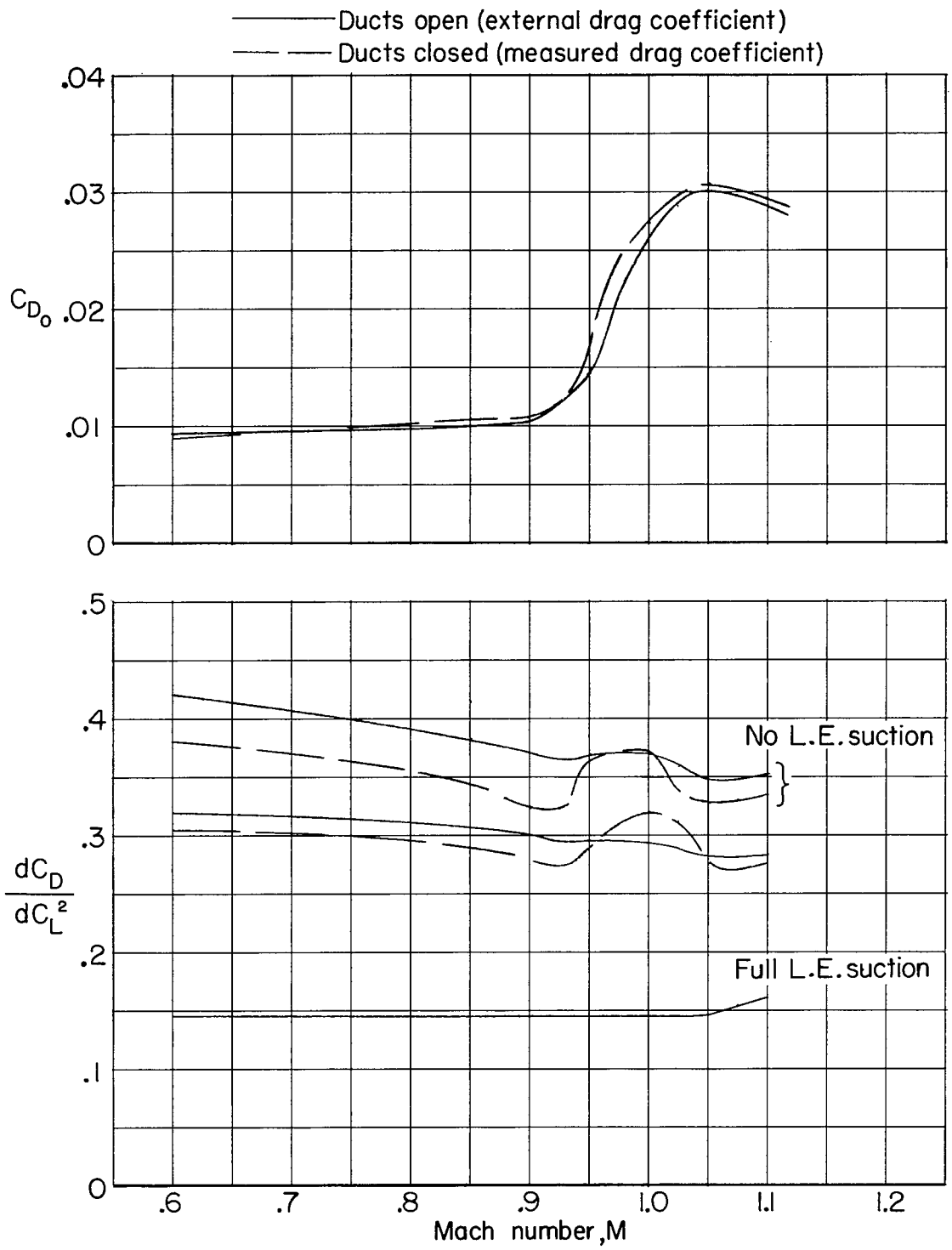

Figure 14.- Variation with Mach number of the drag at zero lift and drag due to lift for the basic configuration with ducts open and closed. Internal drag removed from ducts-open data.

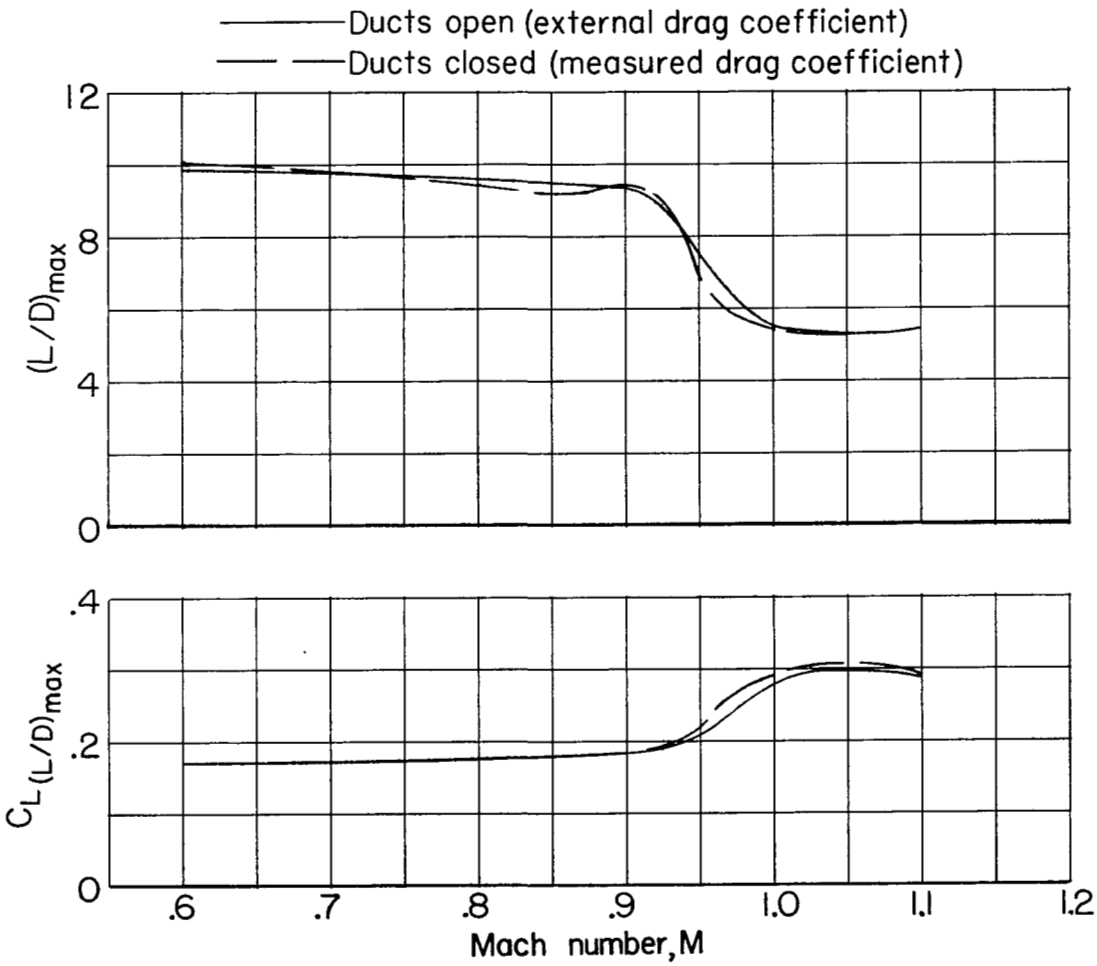

Figure 15.- Variation with Mach number of maximum lift-drag ratio and lift coefficient for maximum lift-drag ratio for the basic configuration with ducts open and closed. Internal drag removed from ducts-open data.

[redacted]

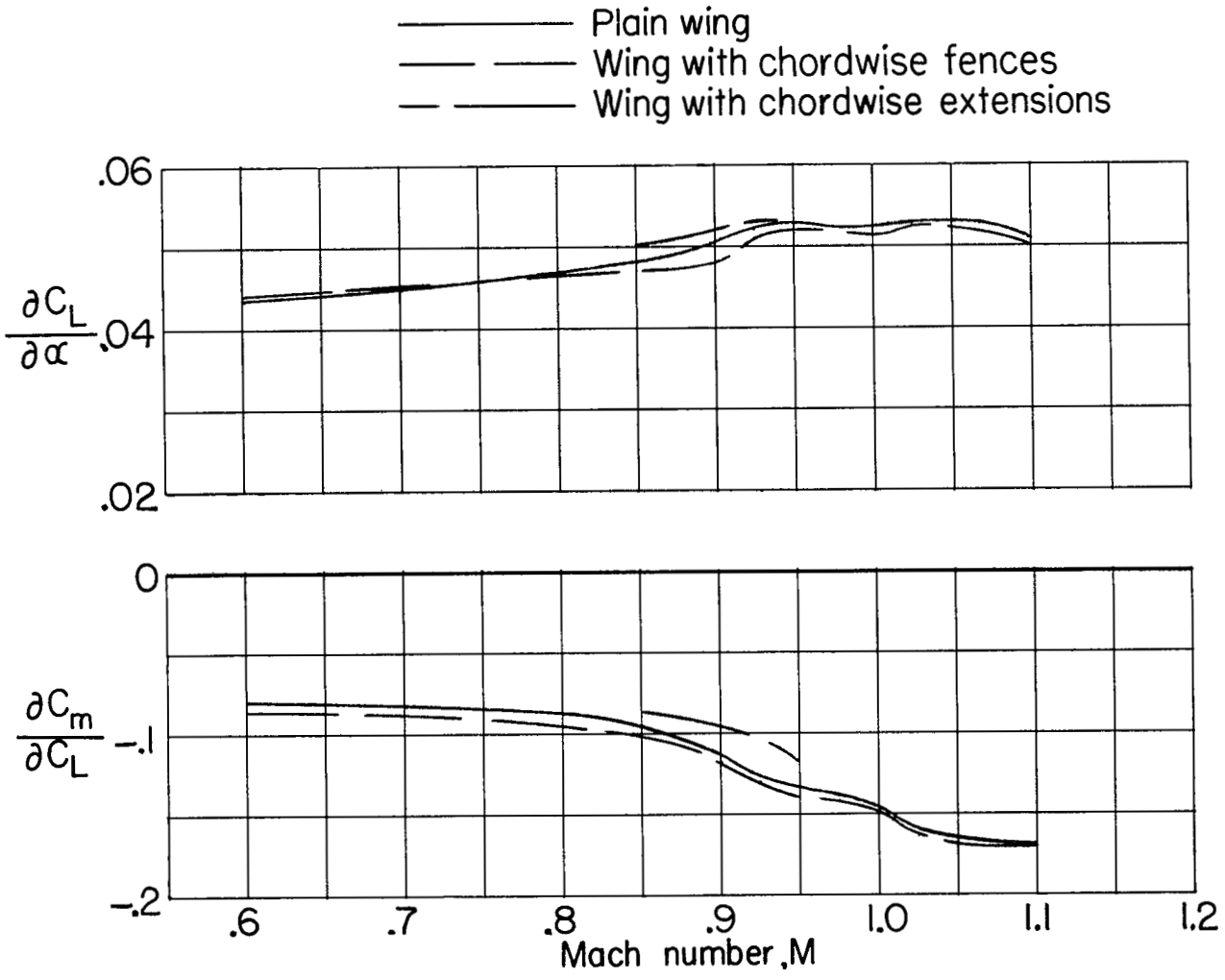

Figure 16.- Effect of chordwise fences and the chordwise extension from 0.6b/2 on the average lift-curve slope and static-longitudinal-stability parameter for the basic configuration with ducts open.

[redacted]

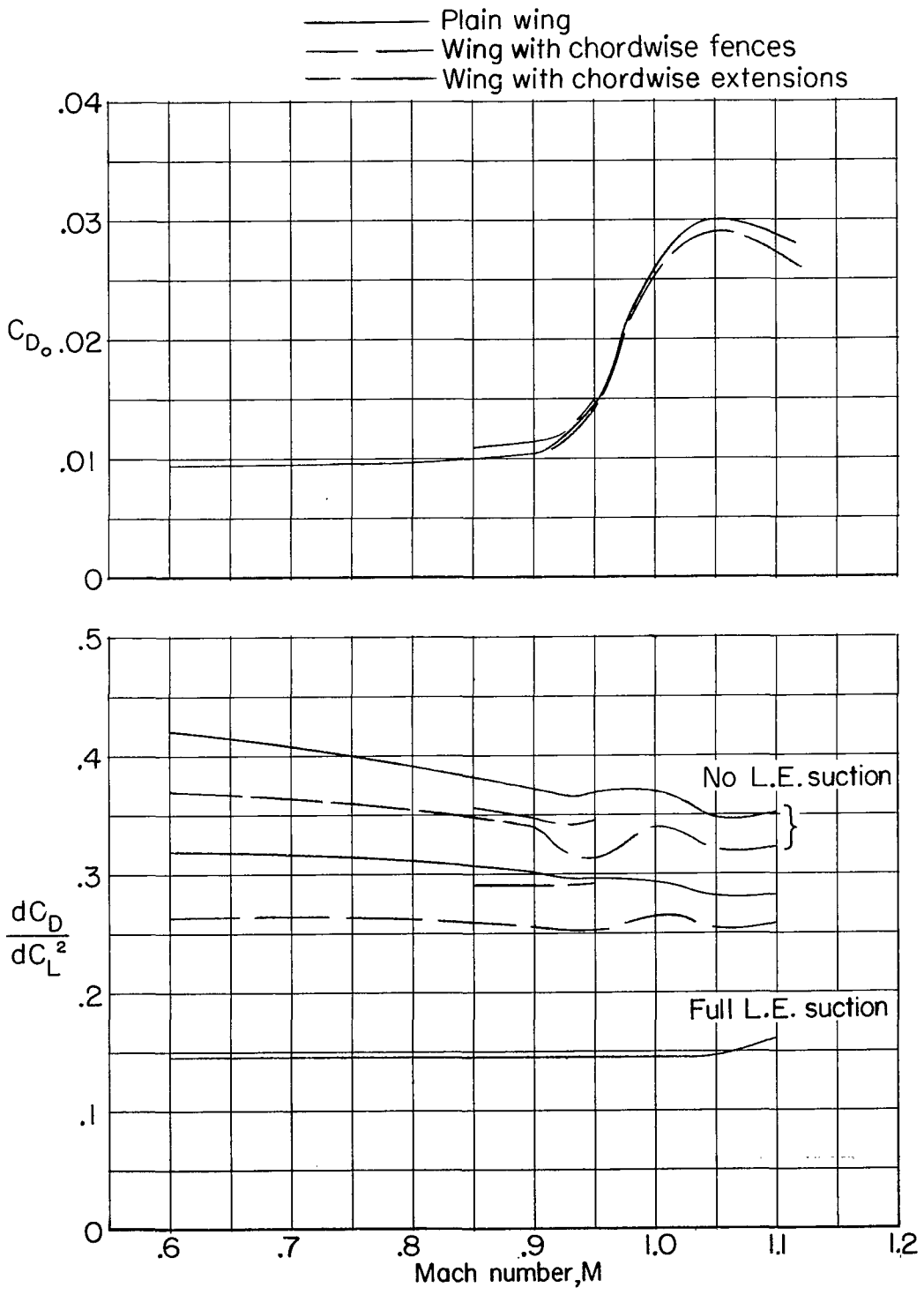

Figure 17.- Effect of chordwise fences and the chordwise extension from 0.6b/2 on the drag at zero lift and drag due to lift for the basic configuration with ducts open. Internal drag removed.

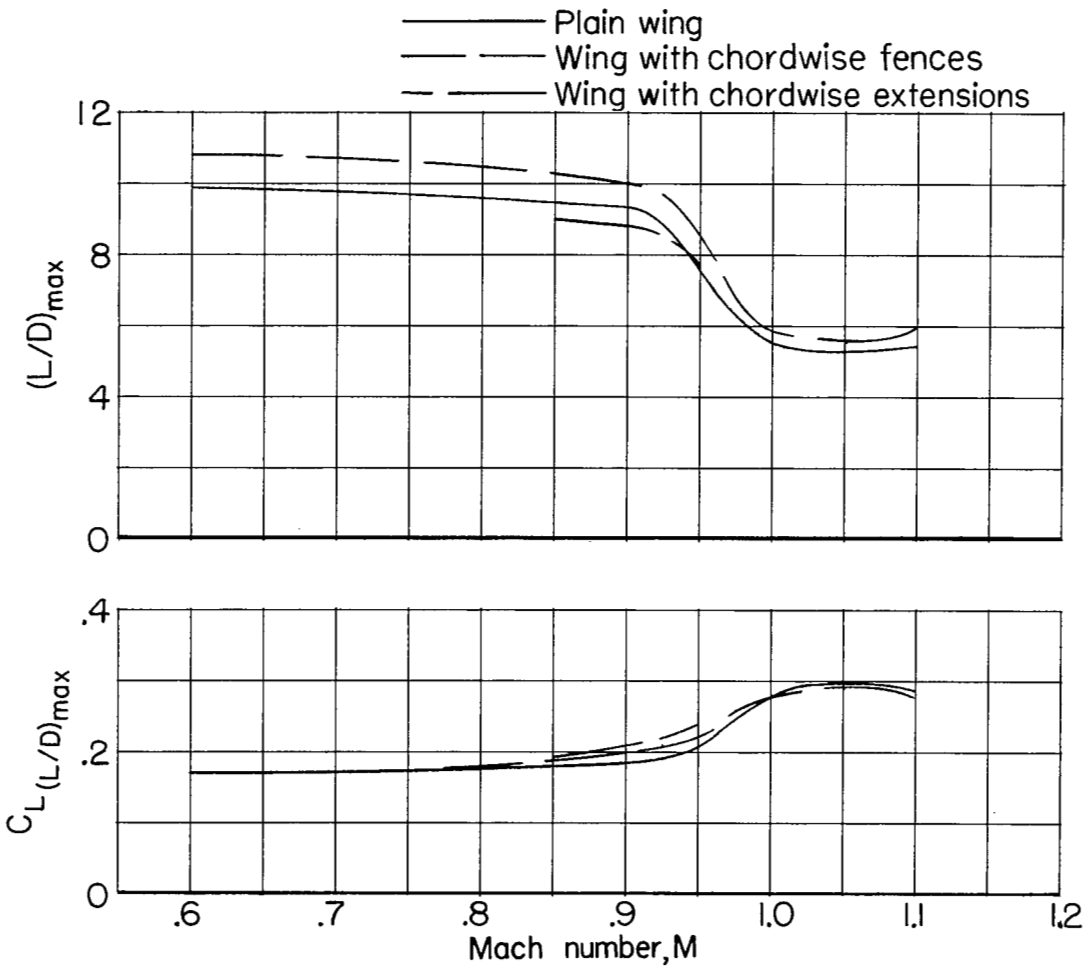

Figure 18.- Effect of chordwise fences and the chordwise extension from 0.6b/2 on the maximum lift-drag ratio and lift coefficient for maximum lift-drag ratio for the basic configuration with ducts open. Internal drag removed.

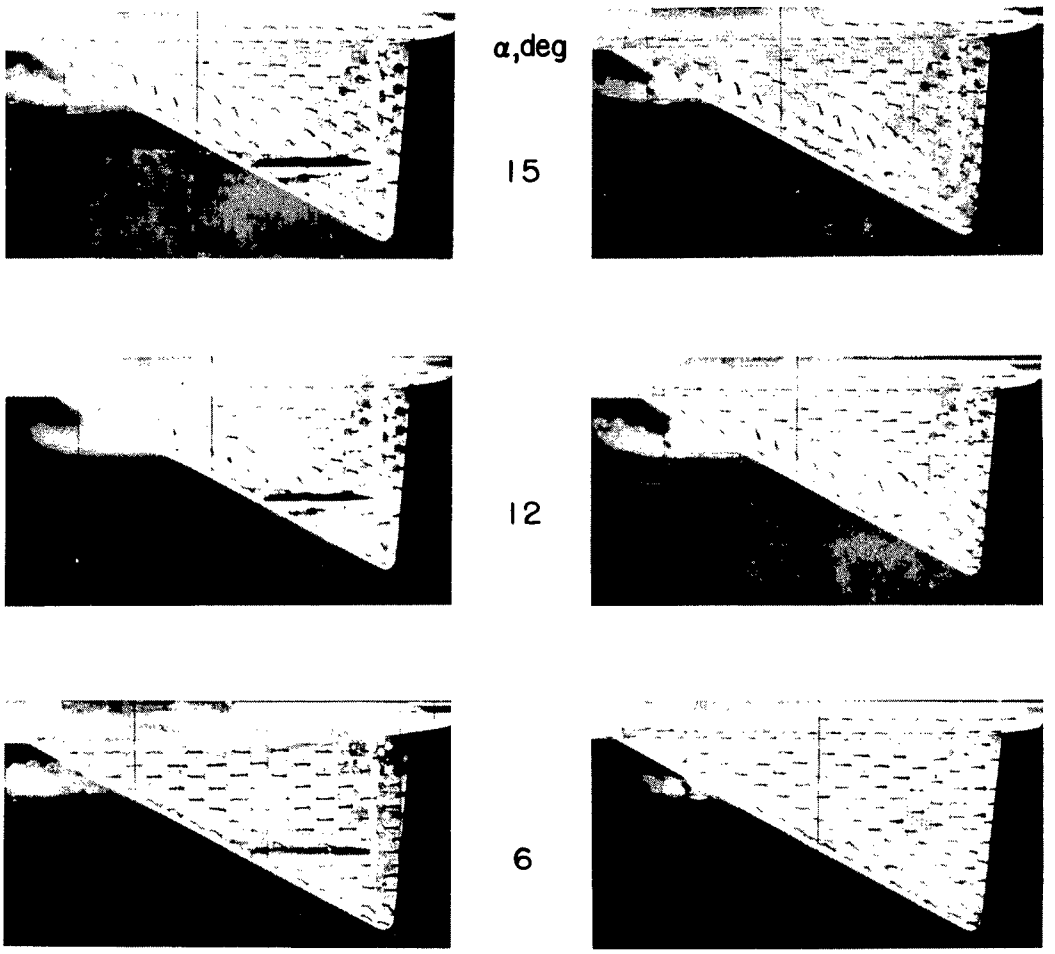

M=0.60.

L-83608

Figure 19.- Tuft photographs for the basic configuration with and without chordwise fences. Ducts open.

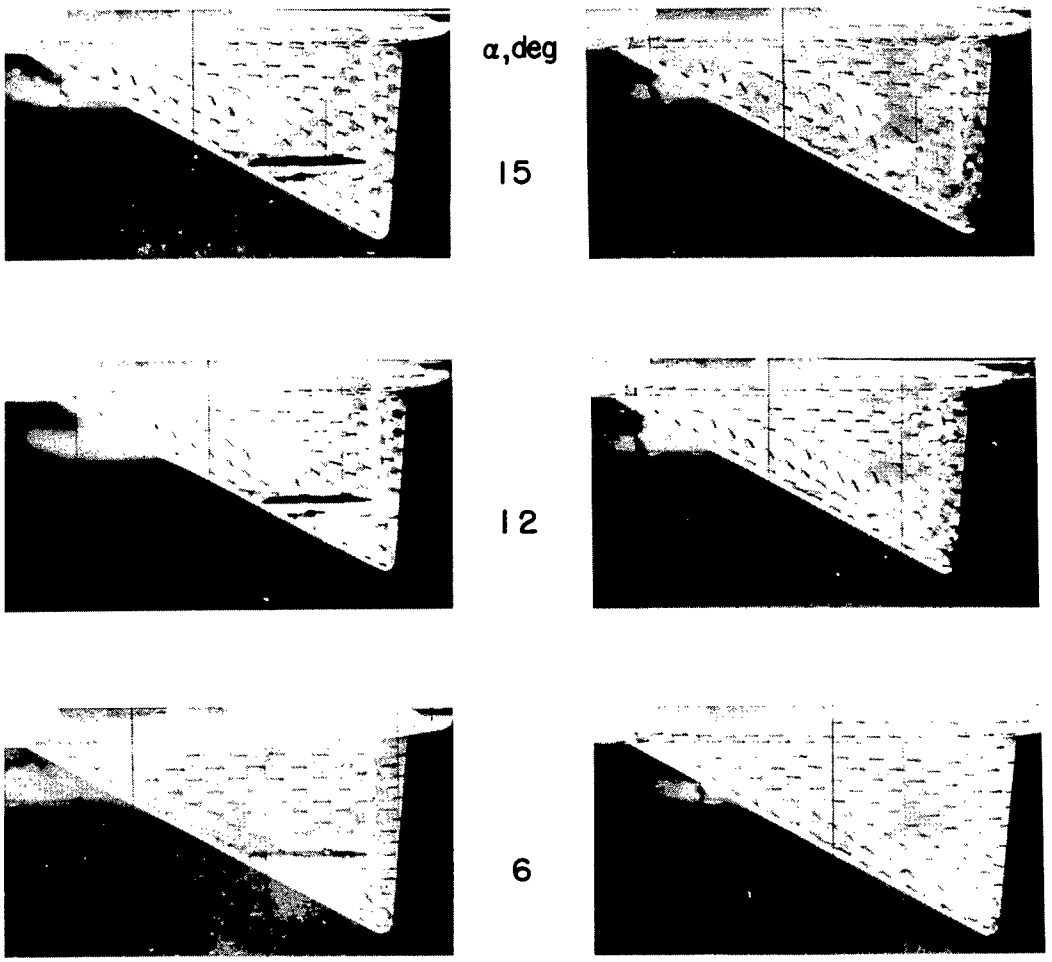

Fences on

Fences off

M=0.90.

L-83609

Figure 19.- Continued.

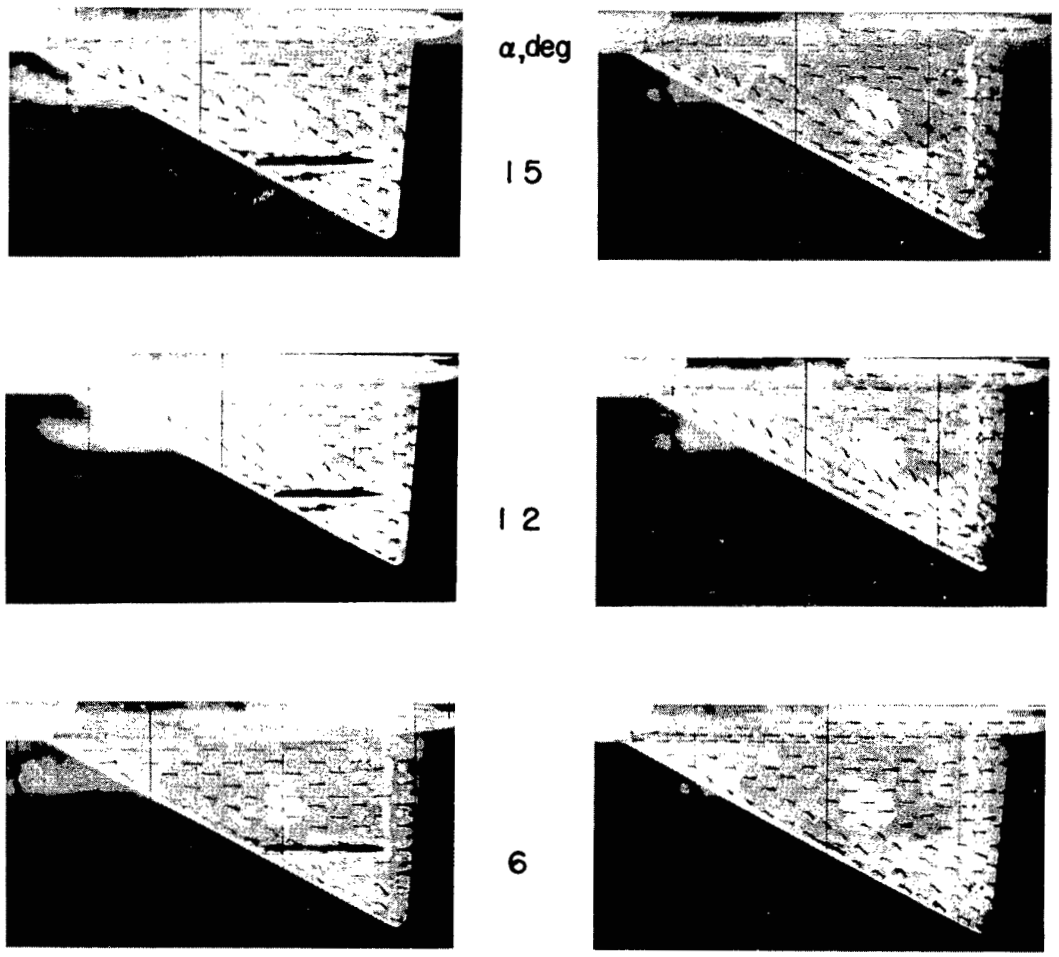

M=1.00.

L-83610

Figure 19.- Continued.

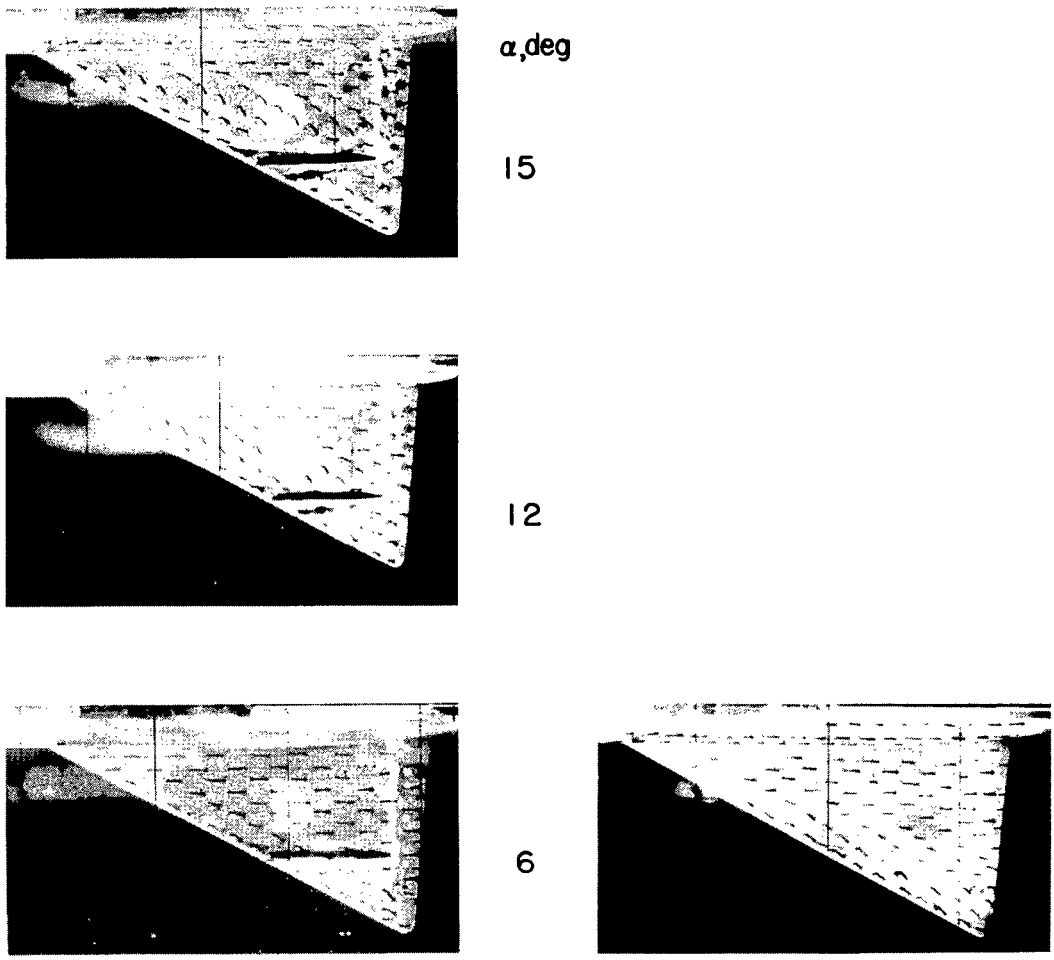

M=1.10.

L-83611

Figure 19.- Concluded.

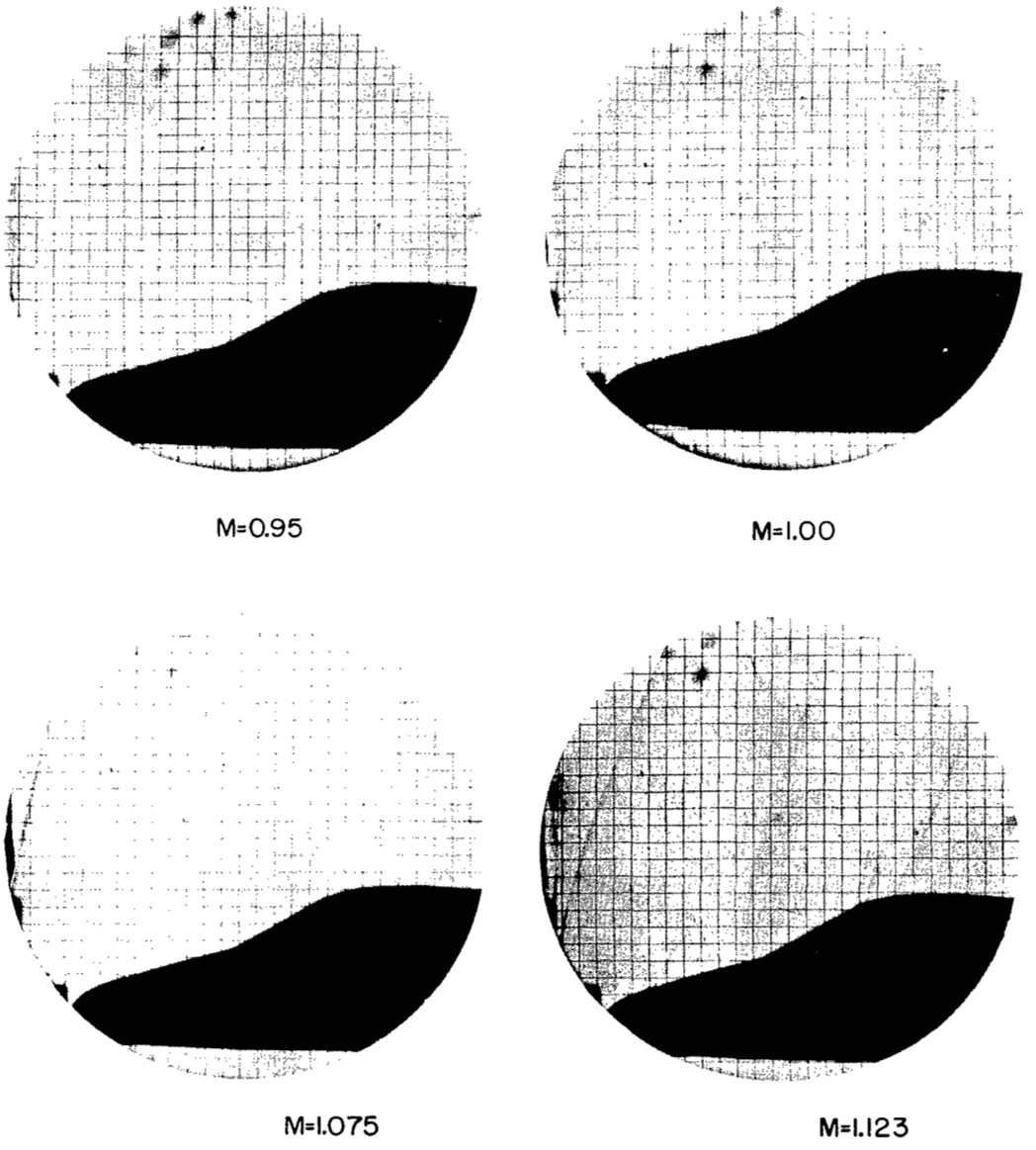

L-83612

(a) Nose section.

Figure 20.- Schlieren photographs of the basic configuration at zero angle of attack. Ducts open.

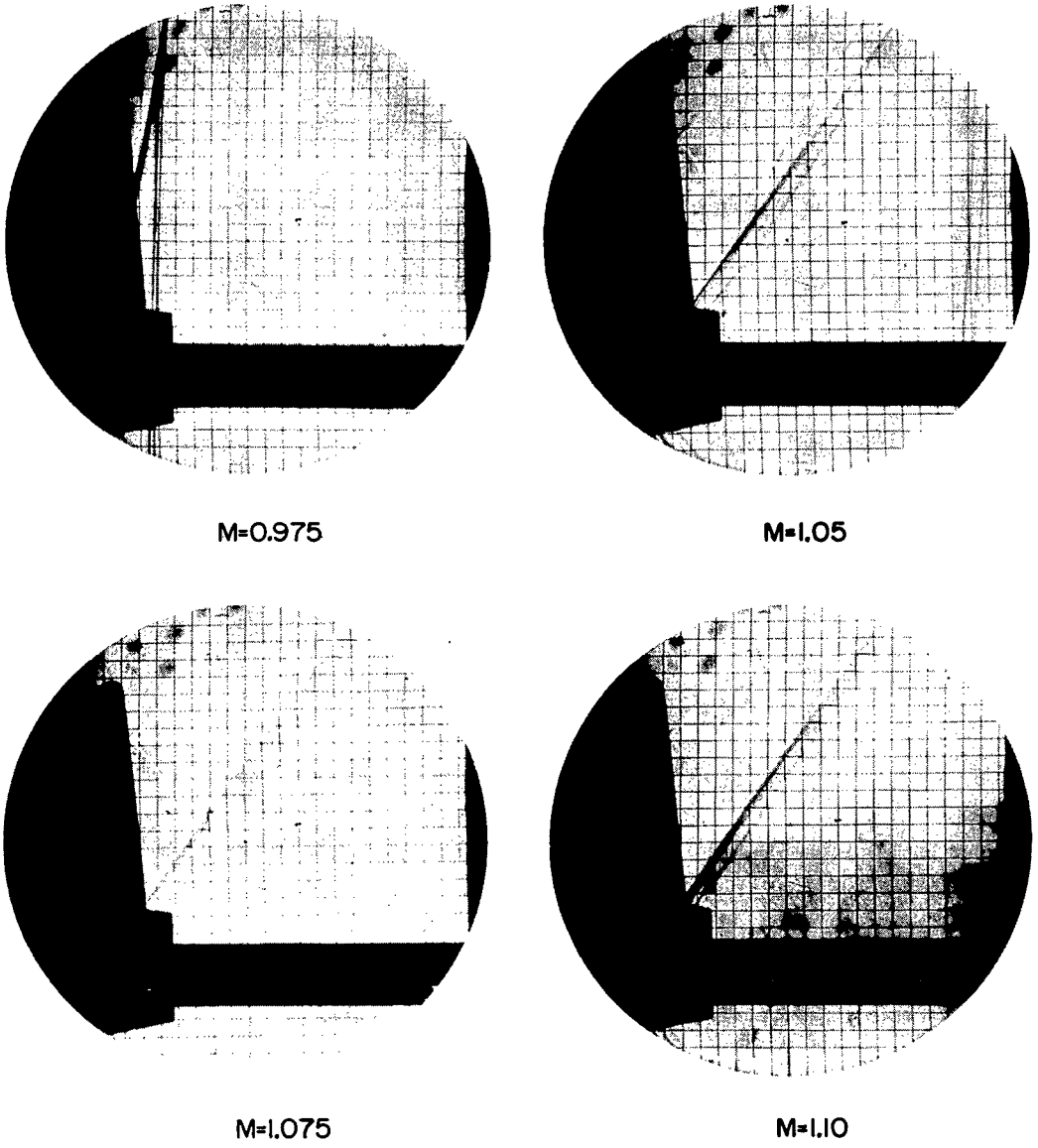

L-83613

(b) Tail section.

Figure 20.- Concluded.